Chapter 11

Environmental Applications of Metal−Organic Frameworks and Derivatives: Recent Advances and Challenges

Adetola Christianah Oladipo,[1] Temitope Olabisi Abodunrin,[1] Deborah Temitope Bankole,[1] Oluwole Solomon Oladeji,[1] Godshelp Osas Egharevba,[1] and Olugbenga Solomon Bello[*,1,2]

[1]Department of Physical Sciences, Industrial Chemistry Programme, Landmark University, Omu-Aran, Kwara State 251101, Nigeria

[2]Department of Pure and Applied Chemistry, Ladoke Akintola University of Technology, P.M.B. 4000, Ogbomoso, Oyo State, Nigeria

[*]Emails: osbello06@gmail.com, osbello@lautech.edu.ng

The consequence of environmental pollution has raised the dire need for the discovery of efficient and potent methods for detection and removal of pollutants released into air and water bodies. Metal-organic frameworks (MOFs) are porous coordination polymers having intriguing features such as large surface areas, tailorable pore size and highly dense active sites reported for various environmental applications. Recent developments have focused on the modification of MOF structures, development of MOF-based materials including functionalized MOFs, MOF composites/hybrids and MOF derivatives. These modifications confer new and desirable properties over pristine MOFs and consequently lead to enhanced efficiency for pollutant sensing and adsorption applications. This chapter focuses on the recent developments and challenges in the use of MOF-based materials for sensing and adsorption of pollutants from air and water in the past seven years. Some challenges and future prospects are also discussed. In spite of the challenges encountered with the use of MOF-based materials for detection and removal of gaseous and water pollutants, they remain valuable materials for environmental applications.

1. Introduction

In recent times, environmental pollution has posed threats to the public and ecosystem. The criticality of this can be seen in the United Nations Sustainable Development Goals (SDG) which has five of her goals centered on the environment for improved standards of living (*1*). Increase in population and industrialization are key players responsible for environmental pollution and this results in the increase in toxic wastes and hazardous compounds in the atmosphere and water bodies (*2*–*5*).

Kumar et al.; MetalOrganic Frameworks for Environmental Sensing
ACS Symposium Series; American Chemical Society: Washington, DC, 2021.

Air pollution has recently become a global subject as a result of rapid industrialization and urbanization (*6*, *7*). Forms of air pollutants include particulate matter, dust, toxic gases, liquid droplets and bio-aerosols which are major threats on human well-being (*4*, *8*). Major air pollutants are oxides of sulfur (SO_x), nitrogen (NO_x), and carbon, chlorofluorocarbons, etc. These molecules have contributed to the formation of acid rain, smog, climate change and damage to ecological systems (*4*, *5*, *9*). Health effects of air pollution are exacerbation of asthma, increased respiratory mucosal symptoms, chronic obstructive pulmonary disease, cardiovascular disease and mortality (*10*).

Sulfur dioxide is a byproduct of fossil fuel emissions and is very toxic. Its presence as a pollutant is significant because trace quantities affect human health and form hazardous $PM_{2.5}$ products having deleterious effects on the environment (*4*, *5*). Exposure to high concentrations results in difficulty in breathing, respiratory illness and aggravation of cardiovascular disease. In the environment, it causes foliar and crop damage, acidification of lakes and streams, acid deposition that accelerates the decay of buildings and monuments also contributes to visibility degradation (*11*). The two major oxides of carbon are carbon monoxide and carbon dioxide. Carbon monoxide is an important feedstock for the synthesis of various chemical compounds. Although a colorless and odorless gas, it is highly toxic to humans and the environment. Exposure to CO leads to unconsciousness, disorientation and death (*5*). A major greenhouse gas is carbon dioxide which is generated from the combustion of fossil fuels (*12*). The major sources of nitrogen oxides are anthropogenic sources such as agricultural activities, automobile exhausts, natural gas, coal and oil burning. Nitrogen oxides are highly toxic and hazardous to humans and are causes of severe environmental challenges. The most common ones present in the atmosphere are nitric oxide and nitrogen dioxide. The effects of exposure to humans are skin irritation, respiratory, nervous and immune damage. While on the environment, it generates acid rain, forms photochemical smog, depletes the ozone layer and increases global warming (*5*, *10*, *13*). Pesticides released through surface runoffs into water bodies damage the flora and fauna, cause diabetes, cancer, asthma, leukaemia and Parkinson's disease (*14*).

Water pollutants either occur naturally or through anthropogenic sources. Some water pollutants found in wastewater are dyes, pharmaceuticals and personal care products (PPCPs), polyaromatic hydrocarbons (PAHs), pesticides, heavy metals and radioactive substances (*15*). These pollutants are from industrial effluents discharge from manufacturing industries (such as food, leather, cosmetics, textile, petrochemical, paper and paint industries), oil spillage during exploration of crude oil, agricultural practices, etc. (*16*) The frequent and extensive use of these products, coupled with their poor removal by conventional wastewater treatment methods have made these pollutants ubiquitous in the environment.

Metals such as Cr(III) and Cr(VI) are mutagenic and carcinogenic due to their acute toxicity (*17*). The presence of Hg(II) leads to loss of vision and hearing, neurological deteriorations and damages to endocrine system (*18*, *19*). Radioactive metals accumulate in living organisms and are highly toxic and carcinogenic (*20*). Dyes are known to cause human health disorders and disturbance in the ecological balance due to their stability to heat, light and oxidizing agents (*21*). Antibiotics which are examples of PPCPs threaten the environment and damage the human central nervous system (*22*). Dibutyl phthalate, an example of persistent organic chemicals (POP) in water effluents, causes disruption of the endocrine, reproductive and nervous systems in humans (*23*).

2. Metal−Organic Frameworks (MOFs)

MOFs constructed from metal ions/clusters and organic linkers were first reported in 1995 (*24*). MOFs are organic-inorganic crystalline hybrid materials which consist of strong bonds between organic linkers and metal ions/clusters. The metal clusters in this case are referred to as secondary building units (SBUs). They form connecting points that are linked together by the organic linkers, resulting in framework formation. The SBUs direct the MOF topology with their intrinsic geometries. The metal ions are locked into their positions by the linkers. This results in high structural stability of MOFs constructed by SBUs (*25*). MOFs are well known for their fascinating properties which include well-ordered structure, tunability, high porosity, diverse functionalities, large pore volume and surface area, good optoelectronic properties, high stability and the possibility to incorporate chemical functionalities without disrupting the framework. These properties distinguish them from other conventional porous solids like zeolites. One of the attractive features of MOF lies in the tendency of its structure to be tailored through modification of chemical nature, activity and surface properties for specialized applications in adsorption, separation, chemical sensing, catalysis, light harvesting, drug delivery, photocatalysis, bio-catalysis, gas sorption/separation, energy storage and conversion, etc. (*26*–*36*)

2.1. MOF-Based Materials

MOF-based materials have arisen due to their intriguing functionalities, tailorable and diversified structures, adjustable morphology, uniform heteroatom doping among others. MOF-based materials sometimes retain and extend the inherent features of pristine MOFs with greater advantages, applications and potentials for better performance. These materials are easily fabricated, increase flux mass transfer and provide easily accessible active sites. They also expose highly dense active sites, optimize size and morphology, and favor structure-performance relationship. The relationship between the morphology, physical and chemical properties of the organic and inorganic building blocks and the species encapsulated inside the pores is responsible for the variety of functionalities exhibited by MOFs (*37*–*44*). The applications of MOFs can be improved by tuning their chemical and physical properties through active groups grafting, change of organic linkers, impregnation of suitable active materials, post-synthetic modification and MOF composite/hybrid formation (*45*).

2.2. Classes of MOF-Based Materials

MOF-based materials are obtained with tailored structures and properties of MOF in pre-design (pre-synthesis) or post-synthetic modification where species, geometry, size and functionality are changed or varied (*38*, *46*). MOFs either retain or sacrifice their backbone to yield various derivatives. Therefore, they can be broadly classified into nanoscale MOFs, functionalized MOFs, MOF composite/hybrid and MOF derivatives.

2.2.1. Nanoscale MOFs

MOFs with at least a dimension in the range of tens to hundreds of nanometers are referred to as nano-MOFs (n-MOFs). n-MOFs have larger surface area, improved dispersibility in aqueous media or other solvents than bulk MOF. MOF nanoparticles possess diverse morphologies such as sphere, cubic and octahedron (*47*). They can be prepared through solvothermal/hydrothermal, microwave assisted, ultrasound assisted, mechanochemistry, microemulsion, continuous flow production

methods. Nanoscale materials are classified into particles, fibers, tubes, rods, thin films and membranes. Synthesis is carried out by controlled precipitation of self-assembled metal-organic polymers and confinement of supramolecular assembly at nanoscopic locations using templates (*48*).

2.2.2. Functionalized MOFs

Incorporation of multiple functionalities into a single network of MOF is of interest in recent times. Functionalization presents an effective strategy for tuning chemical and physical properties (*49*). Several MOF linkers which possess various functional groups such as amine, halogen, hydroxyl, nitro, carboxylic acid, sulfonic acid, among others, have been employed for synthesis to obtain desired functionality (*50*). The methods for functionalization are: Post-synthetic modification and Solvent-Assisted Linker Exchange (SALE) (*1*). Functionalization can be achieved through pre-design/post-synthetic modification of organic ligands or metal ion/clusters, use of functional ligands or metals for construction of frameworks and encapsulation of functional molecules into the pores (*51*).

The synthetic strategies employed for MOF synthesis for optimum design platform for functionalized MOFs involve the tailoring of either organic ligands or metal clusters with multiple functional sites or the introduction of multiple guest components as functional sites or construction of framework with functional sites and guest molecules (*50*, *52*). Their modification can be accomplished before or after the process of synthesis (*50*). In these MOFs, the physicochemical features of each component are superimposed to accomplish an overall performance better than those of the individual components or their adducts (*53*).

2.2.3. MOF Composites/Hybrids

A multi-component material with multiple phases containing at least a continuous phase is known as composite. MOF composites are hybrid materials which comprise of MOF and other suitable constituent materials with noticeably different properties from those of the individual constituent. MOF composites usually combine the advantages of both constituents to get rid of their drawbacks(*54*, *55*). MOF composites originate from the addition of MOF with functional substrates to improve stability and cause increase in adsorption sites (*49*). The integration of MOFs with functional materials such as carbon nanotubes, metal nanoparticles and nanorods, graphene, metal oxides, complexes, enzymes, etc. results in the formation of composites with multifunctionalities and generation of new physical and chemical properties (*38*, *56*, *57*). MOFs can also integrate their large surface area/ high porosity, crystallinity and flexibility along with optical, catalytic or electrical properties of other materials to form composites (*58*). This synergy gives the resulting composite a wider range of applicability than the individual component (*59–61*).

The synthetic method often employed for the synthesis of MOF composites are in situ synthesis and post-synthetic methods. In the in situ method, the composite is obtained by addition of pre-synthesized materials to the solution of the MOF (*57*). The in situ methods are either by bottle-around-ship method or ship-in-bottle method. In the bottle-around-ship method, large particles of composing materials are immobilized inside the cages of MOF via in situ building of MOF from precursors around the composing materials. While in the ship-in-bottle method, the composite is stabilized inside the pores via thermal or chemical methods where the composite materials form and is diffused by a solvent system inside the cages of MOF (*45*). In post-synthetic method, the composites are obtained by absorption of target precursors into the MOFs by immersion and vapor

deposition methods followed by further processing for conversion (*57*). It involves simple loading or impregnation of composing materials in the MOF where the solubility of composite materials are of less concern (*45*).

MOF composites improve adsorption capacity, surface area and ease of separation. The suitability of MOF composites for environmental applications stem from their synthetic kinetics, morphology, physicochemical properties and stability (*49*).

2.2.4. MOF Derivatives

MOF derivatives are obtained by using MOFs as sacrificial templates or precursors. Usually the MOF template/structure backbone is destroyed (*37*, *52*). Generally, the applications of MOFs are limited by their instability and poor conductivity (*62*, *63*). A method designed to address this limitation is by the conversion of pristine MOFs to much more stable materials that can serve as precursors to other porous materials with large surface area (*37*, *64–66*). MOF derivatives are obtained by thermal conversion (*62*, *67*). Their properties include increase in pores, with high surface area and narrow pore-size distribution (*38*, *68*). These derivatives contain any of porous carbon, metal/carbon, metal oxide/carbon, metal/metal-oxide/carbon-based materials, etc. The properties inherited from the parent MOFs are large surface area, uniform heteroatom doping, highly dispersed active sites and controllable compositions (*67*). Features of MOF derivatives are enhanced stability, large surface area, ordered porous structure and ease of pore size adjustment (*39*, *62*, *69*, *70*).

MOF derivatives are commonly prepared using thermolysis, pyrolysis, carbonization and calcination. In thermolysis strategy, the metal nodes are transformed into metal nanoparticles while the organic bridging ligands form highly porous carbon materials (*37*, *39*). Direct pyrolysis is a simple but effective method where metal-free carbons are prepared from MOF subjected to carbonization under an inert atmosphere of nitrogen or argon gas with in situ evaporation and/or subsequent leaching of metal species. In this method, partially preserved morphology is obtained where pyrolysis takes place under air to remove the carbons (*43*). The formation of metal/metal oxide embedded carbon can be obtained by simple pyrolysis of MOF (*68*). Pyrolysis usually enhances the chemical activity and durability of MOFs (*38*). Carbonization at higher temperature yields a higher degree of graphitization (*66*). Carbonized MOFs consist of both metal and carbon sources. Hybrid structures such as carbon-supported metal/metal oxides and hybrids from different metal-based compounds containing more than one component are prepared under inert atmosphere by direct carbonization of MOFs (*38*, *43*). This process can take place with or without a secondary carbon. The nature of the carbonized material depends on the rate of heating, temperature of calcination, crystal size and component of MOF (*38*). Calcination yields porous carbon when the MOF is subjected to heat in air or an inert atmosphere at elevated temperatures over time (*57*, *69*). This chapter explains the use of MOF-based materials for environmental applications. Specifically, the sensing and adsorption of several gaseous and water pollutants using MOF-based materials are discussed. The efficiency, mode of action of the materials for the various applications and chemical interactions between the sensors/adsorbents and the pollutants are reviewed.

3. Environmental Applications of MOF-Based Materials for Sensing of Pollutants

The hazardous effects that toxic pollutants have on the environment and human health make their detection necessary. The detection of pollutants is imperative for air monitoring and subsequent removal. Sensing materials, capable of rapid and selective detection of toxic species are required

for this purpose. Several technologies have been employed for sensing of organic and inorganic pollutants (*71*). Some of these conventional methods are configured with high sensitivity and accuracy. However, they require expensive equipment, and the needed pre-treatment of water samples is highly complicated. Compared to conventional detection methods, the use of materials as chemical sensors is simple, economical and useful in real-time monitor (*72*). The operation of chemical gas sensors is based on the changes of some properties as a result of their interaction with analytes. MOFs are a relatively new burgeoning class of materials for gaseous and aqueous phase sensing. Measurable changes in intrinsic properties, when exposed to target analytes, qualify MOFs as sensors.

The fascinating and desirable properties possessed by MOFs make them suitable candidates for sensing applications: the porosity of MOFs enables the adsorption/desorption of guest molecules, in this case, the analyte to be sensed. Selective sensing capability for target analyte is made possible by the tunable pore size of MOFs. The pore dimensions of MOFs are modulated to allow the target analyte molecule to be included. Coordinatively unsaturated sites (CUS) created by the removal of occluded solvent molecules could be used to capture guests and enhance selectivity by reversibly binding with the target analyte (*73*).

The earliest MOFs synthesized were in form of bulk crystalline materials and are restricted by poor dispersibility in solution. These MOFs have limited applications in sensing pollutants, especially in aqueous solution. In recent times, nanoscale MOFs (n-MOFs) with larger surface areas than conventional MOFs have successfully overcome the barrier faced by conventional MOFs. The larger surface areas and more accessible active sites in n-MOFs, result in better sensing capability (*48*).

The water stability of MOFs is an essential property in selecting MOFs for sensing applications. It was acknowledged that MOF frameworks are destructible at the preliminary stage of synthesis since the ligand–metal bonds in the MOFs are easily susceptible to attack by water molecules. This barrier has been crossed by the introduction of water stable MOFs. Two of the categories according to their mechanism of formation, are stated as follows: First is the metal carboxylate frameworks consisting of high-valence metal ions, like Cr^{3+}, Fe^{3+} and Zr^{4+}. These ions possess high coordination number and charge density, which enhance the stability coordination bond of MOFs between metal ions and ligands. The second type is metal azolate frameworks comprising nitrogen-donor ligands, like tetrazolates, imidazolates, pyrazolates, and triazolates. The nitrogen-containing ligands are typically soft ligands, which can react with soft divalent metal ions to form MOFs with strong structural framework (*74*).

Incorporating additional functionality on the ligand, or nanoparticles into the accessible volume of the pores could also be a strategy to achieve selectivity (*75*). Metal oxide semiconductors derived from the pyrolysis of MOFs have also been reported to have large surface areas and surface active sites which offer advantages like high response, low working temperature, and low limit of detection in sensing applications (*72*).

3.1. Transduction Schemes for MOF-Based Sensors

The broad classification of MOF-based sensing techniques is based on the employed transducers. A transduction unit translates the sensed information from the sensing unit into a signal. The mode of action of the sensor is based on the transduction mechanism (*76*). Sensing in MOFs could be through optical, mechanical and electrical methods as shown in Figure 1.

The optical methods involve changes in color, luminescence features and refractive index. The emission of photon when the excited electron returns to the ground state is called

photoluminescence. This emission could either be quenched or enhanced on exposure to an analyte. This depends on the extent of the host-guest interaction. Also, there could be shifts in the emission frequency. This is useful in the detection of analytes, in addition to the emission quenching or enhancement. Analytes with good electron donors or acceptors are easily detected in this case (*77*). Luminescent lanthanide-based MOFs have aroused great interest for use in sensing applications owing to their outstanding luminescent properties. Some of the properties include huge stokes shift, extensive fluorescence lifespan and sharp line emission (*78*). The chemosensing potentials of Ln-MOFs have been widely explored on organic small molecules and nitro explosives (*79*, *80*).

In chromism, there is a reversible change in color upon adsorption/desorption of analytes either in solution or gaseous state, these are termed solvatochromism and vapochromism respectively. The chromophore electronic transition from ground to excited state causes a large shift of the absorption spectrum which accompanies the change in color of the sensing material. In addition, there could be color change, resulting from the change in the coordination environment of the metal centers in the MOF.

Interferometry involves the measurement of the change in the refractive index on exposure to target analytes. This is done by monitoring the shifts of the interference peaks in the transmission spectrum. In this case, the MOF material has to be in form of thin film and the reflective surface on both sides of the film (*81*).

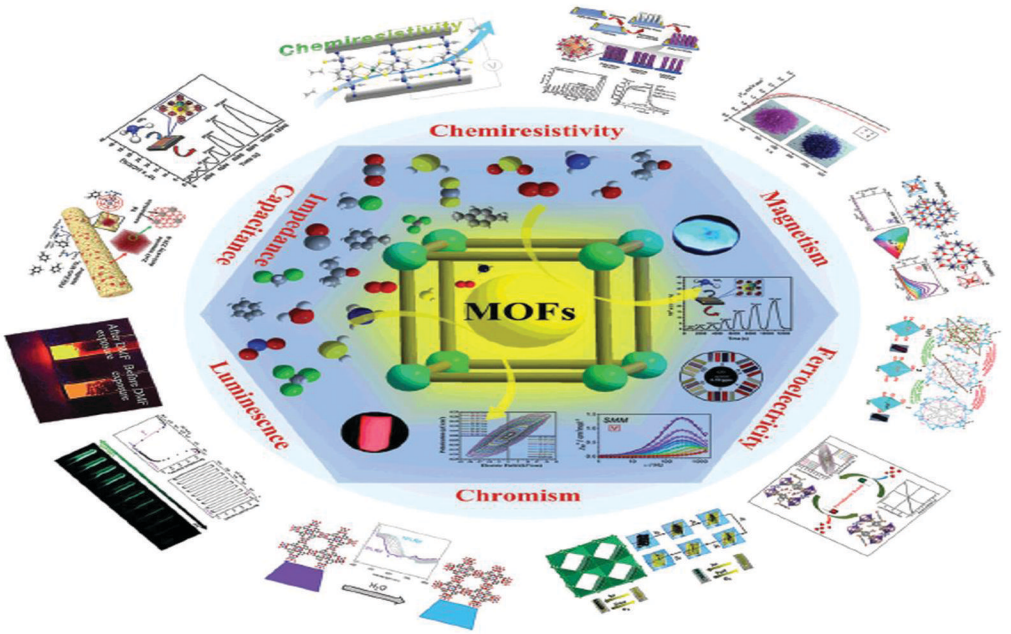

Figure 1. Sensing based on MOF properties. Reproduced with permission from reference (*82*). *Copyright 2020 Royal Society of Chemistry.*

Mechanical methods involve the absorption of analytes by MOF grown on electromechanical devices such as surface acoustic wave sensors, microcantilevers (MCL) and quartz crystal microbalance (QCM). These devices can convert gravimetric changes into vibrational signals. The gravimetric changes influence the frequency of acoustic waves, cantilever and resonant vibrations of the quartz crystal respectively, resulting into signal generation and detection (*82*).

The electrical method involves the reaction of target analytes with oxygen in the environment and detecting the changes in the electrical properties such as impedance, capacitance, work function and resistance (*83*). Here, the reaction of the target analyte with oxygen adsorbed on the surface of the MOF material at high temperature is required. The high porosity of MOFs is beneficial in the conductivity-based sensing applications (*84*).

Some recent exciting examples in the application of MOF-based materials in the detection of both gaseous and water pollutants are discussed in the subsequent section.

3.2. MOF-Based Materials for Sensing Gaseous Pollutants

The detection of volatile organic compounds (VOCs) from emission sources at working and residential places is important. The fabrication of capacitive sensor based on Cu-1,3,5-benzenetricarboxylic acid (BTC)MOF-199nanoporous film and coated on a copper substrate, was reported for the detection of ethanol, methanol, acetone and isopropanol vapors. The sensitivity was in the range of 250-1500 ppm and the sensor offered a reasonable response time and reversible detection of the analytes. Factors that affected the sensing ability for the different analytes were the dielectric constant, concentration of the analytes and the extent of adsorption into the MOF film (*85*). The same research group also reported that low limit of detection of 130.0 and 39.1 ppm for ethanol and methanol was obtained with the use of the same nanosensors. The reusability of the sensor for several sensing cycles was possible due to its reversible affinity toward the vapors of the analytes. There was selective sensing of the polar analytes over non-polar n-hexane (*86*). A zinc-based MOF was pyrolyzed to yield hierarchical hollow ZnO nanocages possessing hollow interiors covered by interpenetrated ZnO nanoparticles. It provided mesopore and macropore channels which aid the diffusion and subsequent reaction of gas molecules. The large surface area and exposed active sites offer a highly sensitive sensing toward acetone and benzene. The high sensitivity toward the VOCs, in sub-ppm and ppb levels, was attributed to the surface-adsorbed oxygen for the oxidation of the reducing analytes, thereby enhancing the sensing of the analytes (*87*). In an attempt to improve the sensing activity of the MOF 5-derived ZnO, the same research group synthesized Au@ZnO heterostructure by the pyrolysis of Au@MOF-5. The core-shell Au@ZnO nanoparticles showed a response value of 11 times higher than what was observed for just ZnO nanoparticles in the sensing of acetone. It was documented that Schottky junction formed by the Au-ZnO interface led to the enhanced acetone-sensing property of the Au-ZnO heterostructure (*87*). In another report, affinity layers were derived by the dispersion of NH_2-MIL-53(Al) nanoparticles in a Matrimid polymer matrix. The composite was deposited on aluminum electrodes and applied for the gas phase sensing of some alcohols. There was a fivefold increase in methanol sensitivity of the MOF composite device as compared to only the polymer-coated device. Increase in MOF concentration also increased the response time (*88*). Ghanbarian et al. developed a ternary nanocomposite of a bimetallic MOF, MIL-53(Cr-Fe), silver, and carbon nanotube (CNT) for the fabrication of a resistive gas sensor to detect isopropanol, ethanol and methanol at 25°C and 10% relative humidity. The analyte for which it had the highest response was methanol, with limit of detection (LOD) of 30.5 ppm. The sensing mechanism could be explained by the flexibility and reversible expansion of MIL-53 with the presence of analytes which led to the increase of the sensor resistance. The CNT helped with electron transport and tunable reactivity while silver spread electron through the composite and increased the conductivity. The conductivity decreased on exposure to the analytes (*89*). In another report on the sensing of methanol vapor, Zn-MOF of benzenedicarboxylate ligand having $Zn_xO_yC_z$ SBU, was synthesized and made a composite with manganese oxide. Although the crystallinity of the Zn-

MOF was sacrificed and the electrical resistivity lowered on addition of MnO_2, the composite could detect methanol vapor (*90*). In another report, double strategy was used for the modification of a Zr-MOF. It was functionalized with a sulfone group and also embedded with a noble metal, palladium to give Pd@Zr-BPDC-SO_2 (dibenzo[b,d]-thiophene-3,7-dicarboxylate5,5-dioxide). The composite was effective in ethanol sensing as a result of hydrogen bonding between the –OH group of ethanol, sulfonyl and Zr_6 clusters (*91*). Cao et al. reported on the preparation of Fe-doped ZnO lattice and the subsequent heterojunction formation with $ZnFeO_4$ nanoparticles. The acetone sensing of the heterostructure surpassed that of pristine ZnO in terms of response time, selectivity, sensitivity and stability. This was attributed to the large surface area, heterojunction formed and abundant adsorption sites for oxygen and analyte molecules (*92*). In a report that involved the study of the effect of carbonization conditions of zeolitic imidazolate frameworks (ZIFs) on surface area and the consequences on selective sensing of VOCs, it was observed that CNT grew on the surface of the nanoporous carbons after carbonization under hydrogen gas atmosphere. The CNT acted as π-rich antennae for the selective sensing of benzene and toluene vapors over n-hexane despite the fact that the high surface area of the CNT-free NPCs was sacrificed with the growth of CNTs. The enhanced and selective sensing of the aromatic hydrocarbons was as a result of the resulting π- π interaction between the aromatic rings of the hydrocarbons and the π-rich CNT (*93*).

The detection of CO_2 gas is paramount in air quality control. Therefore, highly sensitive sensors are required. Gassensmith et al. reported a γ-cyclodextrin-derived material, CDMOF-2, with high proton conductivity and free primary –OH group capable of reacting with CO_2 gas to form alkyl carbonate. This reaction brought about approximately 550-fold reduction in its conductivity. This positioned the material for selective CO_2 sensing by electrochemical impedance spectroscopy (*94*). Nanoporous Cu-BTC was used to develop an ultra-short near-IR fiber optic CO_2 sensor at wavelength of 1.57 μm. It had a rapid response time of 40 seconds and its limit of detection was 500 ppm. It was found suitable for the detection of the greenhouse gas (*95*). MOF analogs of M-MOF-74 (M- Mg, Ni, Co and Zn) and ethylenediamine functionalized Mg-MOF-74 were synthesized and employed for the selective sensing of CO_2 gas by monitoring the change in the work function of the sensing layer. The MOFs could interact with CO_2 gas through the coordinatively unsaturated metal centers. In addition, the NH_2 functional group also interacted with the gas, in the case of the functionalized Mg-MOF-74. Its sensitivity, stability and reversibility positioned it as the best of all the MOF materials used (*96*). In another report, ZIF-8 nanoparticles were integrated onto bimodal optical waveguides for the fabrication of an optical sensor for CO_2 detection. LOD of 3130 ppm at room temperature with a broad linear response was exhibited by the ZIF-8 nanoparticle sensor. There was no loss in performance of the sensor even under humid condition. Furthermore, its robustness, reusability and target analyte selectivity over water vapor and methane made it ideal for CO_2 sensing (*97*). Ye et al. employed impedance measurement for the detection of CO_2 using Zn-MOF-74 and NdMo-MOF. Increase in impedance was observed upon exposure to an increased concentration of CO_2 gas. With the use of Zn-MOF-74, there was a significant rate of CO_2 adsorption but a slow desorption. The rapid response to CO_2 was evidenced by the increase in the real part and decrease in the imaginary part of the impedance (*98*).

Over the years, metal oxide semiconductors like ZnO, TiO_2, SnO_2, etc. have found application in the detection of CO gas with high response. Many metal oxides derived from MOFs have also been used. In a report, n-type semiconductor SnO_2 nanoparticles was derived from a Sn-MOF and

composited with molybdenum diselenide nanoflowers. Selective sensing of CO over other gases like SO_2, CH_4, H_2S, H_2 and even CO_2 was documented. As both SnO_2 and $MoSe_2$ are semiconductors, n-n heterojunction could be formed at the SnO_2 nanoparticle - $MoSe_2$ nanoflowers interface as electrons from $MoSe_2$ with high Fermi level were transferred to SnO_2 with low Fermi level until equilibrium was reached (*99*).

A lot of sensors developed for SO_2 sensing could only be used for its liquid phase detection (*100*, *101*). Its gaseous phase detection is paramount as it is a class of air pollutants. Most reported luminescent Ln-MOF were obtained in powder form, which when applied in solution could be hard to recycle, unsuitable for use with gas flux blast and the dispersion could be time-consuming (*102*). As an improvement to overcome these drawbacks for the sensing of SO_2 gas, MOF-based sensors for SO_2 were developed. Chernikova et al. reported on SO_2 detection using an Indium-MOF (MFM-300). This was coated on a functionalized capacitive interdigitated electrode for the fabrication of a chemical capacitive sensor. This was the first MOF-based SO_2 sensor and coincidentally gave the lowest sensitivity at room temperature, compared to other sensors. The LOD was estimated to be 5 ppb. Furthermore, the sensor was exceptionally stable and reused for several sensing cycles. The selectivity over other gases like NO_2, CH_4 and H_2 was shown by the signal intensity for the target gaseous analyte compared to those of the other gases (*103*). Also, Eu(III)-organic framework film fabricated on UiO-66-NH_2 (UiO- University of Oslo) was developed. Upon the exposure of SO_2, the strong Eu^{3+} emission was rapidly quenched in just six seconds with LOD of 0.65 ppm due to the charge transfer from the occupied π-orbital of the ligand and the empty SO_2 orbital (*104*). Ingle et al. reported a MOF composite made up of Ni_3BTC_2 and OH-functionalized single walled carbon nanotubes (OH-SWNTs). The composite was drop-casted on gold micro electrode tip on Si/SiO_2 substrate. The composite gave a better performance in sensing SO_2 gas than pure Ni_3BTC_2 as measured by its increased sensitivity, fast response time and repeatability at room temperature (*105*). In another report, $ZnFe_2O_4$, derived from a Zn/Fe MOF, was functionalized with rGO. The formation of a p-n heterostructure between the two materials and the good electrical properties of rGO led to a better transient response, sensitivity and selectivity for the detection of SO_2 gas by the $ZnFe_2O_4$/rGO composite compared to single $ZnFe_2O_4$ and rGO (*106*).

For the detection of H_2S gas, malonitrile-functionalized ZIF-90 (MN-ZIF-90) which is a polymeric fluorescence probe, was synthesized. The fluorescence intensity was enhanced with the incorporation of malonitrile when exposed to H_2S gas. This aided the sensing ability of the material (*107*). Also, four MOF materials, including MIL-101(Cr), MIL-100(Fe), ZIF-8 and $Zn_3(BTC)_2.12H_2O$, were used for the development of cataluminescence sensors. After some experiments, the last two MOF materials were outstanding for good sensitivity and stability for H_2S sensing (*108*). A MOF based on rare-earth metal and fumarate ligand was fabricated into thin films on a capacitive interdigitated electrode. LOD of 5 ppb for H_2S detection was obtained. More interestingly, the sensor was selective for the target analyte over other gases like CH_4, NO_2, H_2 and C_7H_8 (*109*). In a report by Zhang et al., the poor selectivity and high working temperature of γ-Fe_2O_3 was addressed by making its composite with reduced graphene (rGO). γ-Fe_2O_3 was derived from MIL-88 and dispersed on reduced graphene oxide. Better sensing performance of the composite than γ-Fe_2O_3, even at room temperature, was as a result of the bulk resistance effect of γ-

Fe_2O_3, good conductivity and much active sites of rGO. The composite offered H_2S selectivity over $CHCl_3$, NH_3, SO_2 and HCHO (*110*). Ali et al. reported the fabrication of MOF-polymer mixed matrix for H_2S gas detection at room temperature. The introduction of MOF-5 led to the sensitivity of the composite to H_2S gas and was attributed to the increase in the surface area of MOF-5 with a special cage-bridge structure which enhanced energy transport. The fast response and high sensitivity (<8 s and 1 ppm respectively), coupled with the room temperature application, made the composite ideal for industrial applications (*111*).

The electrical method of sensing of NH_3 based on changes in normalized resistance was carried out using a MOF hybrid composed of Cu-BTC and either of graphite oxide or aminated graphite oxide. The chemical reaction of the analyte and the MOF component, evidenced by the irreversible increase in resistance upon exposure to NH_3, resulted in the structural collapse of the MOF component. Nevertheless, the electrical signal recorded as the amorphous phase adsorbed the NH_3 gas (*112*). The conductivity measurement of four MOF analogs synthesized from trimesic acid and either of Ba(II), Cd(II), Pb(II) and Zn(II) was carried out before and after exposure to NH_3 vapor. The Zn(II) analogs exhibited about 50 times increase in conductivity after exposure to NH_3, making it an ideal candidate for NH_3 sensing (*113*). Also, Zhang et al. documented the introduction of Eu^{3+} ions to the free carboxylic sites of MIL-124 to obtain MIL-124@Eu^{3+} as a luminescent MOF film. The MOF film was prepared on porous α-Al_2O_3 ceramic plate. In this case, NH_3 gas reacted chemically with the carboxylic group and formed the $-COONH_4$ moiety. The characteristic emission of MIL-124@Eu^{3+} was quenched by the transfer of energy between the ligand and the Eu^{3+} ion as a result of the effect of the resulting $-COONH_4$ moiety. The sensor was chemically stable, as confirmed by XRD analysis (*114*). Another vapoluminescent Eu-MOF was reported for the naked-eye sensing of NH_3 vapor. The solid sample, upon exposure to NH_3 and HCl vapor, exhibited a recyclable on-off-on sensing of the analytes. When viewed under UV light, it was noticed that the red luminescence of the MOF material which turned blue upon exposure to HCl vapor, was regained after being exposed to NH_3 vapor. To gain insight into this response, control experiments were performed and it was believed that the dissociation of Eu^{3+} from the Eu-MOF with exposure to the acidic HCL vapor, was reformed after exposure to the basic NH_3 vapor (*115*).

Two series of isoreticular Mg-MOFs with high thermal stability and large surface area were employed in the detection of NO_2 gas. The resistance of the gas sensor was monitored and found to decrease in the presence of NO_2 gas. The Mg-MOF with the larger surface area had more adsorption sites and adsorbed target gases, which in turn led to more change in resistance and sensor response. It was also documented that the pore size of the material had a great effect on the kinetics of the gas sensor (*116*). MOF analogs of lanthanide ions Eu^{3+} and Tb^{3+} were also explored for the luminescent sensing of NO_2 gas. The inclusion of the gas into the framework led to the increase and decrease in the luminescence intensity of Eu^{3+} and Tb^{3+} MOFs respectively. This was attributed to changes in the relative position of the ligand triplet and the Ln energy levels when NO_2 was adsorbed. Although the interaction between NO_2 gas and the MOF was weak, there was a high sensitivity of the MOF for the target analyte due to the affinity of the amino functional group to NO_2 gas (*117*).

For the chemiresistive sensing of acidic gases SO_2, NO_2, CO_2, pore surface functionalization of Zr-based UiO-66 MOF was explored by the modulation of the terephthalate ligand with the –OH and NH_2 groups (Figure 2). Pristine UiO-66, NH_2-UiO-66, OH-UiO-66 and NH_2-OH-UiO-66 were synthesized and the changes in their electrical resistance on exposure to the acidic gases were monitored. The basic NH_2-UiO-66 offered strong active sites for the acidic gases. Also, the interaction between the basic MOF and the acidic analytes led to a change in the electronic property of the sensing material (*118*).

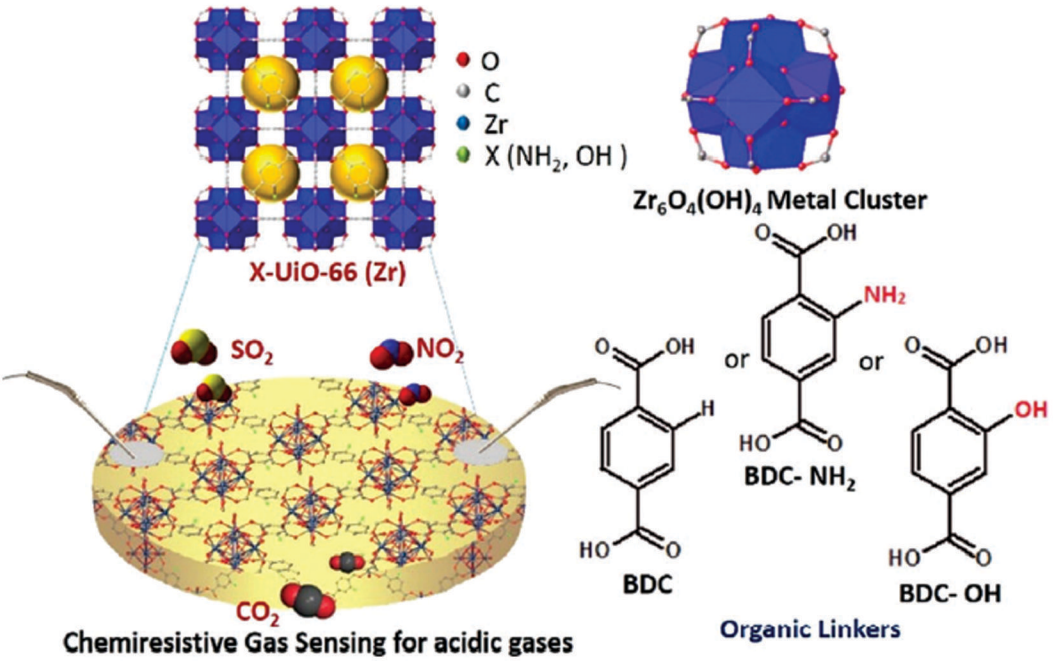

Figure 2. Illustration of chemiresistive sensing of acidic gases by the functionalization of organic linker in UiO-66 MOF with -OH and -NH_2 groups. Reproduced with permission from reference (*118*). *Copyright 2019 Royal Society of Chemistry.*

3.3. MOF-Based Materials for Sensing Water Pollutants

Among all the sensing techniques for MOFs, the luminescent technique is the dominant for cations detection. Luminescent MOFs have found a vast usage for the detection of toxic metal cations in water. Bhattacharyya et al. synthesized an anionic Mg-MOF with very interesting property. It contains cationic dimethyl ammonium (DMA) which could be replaced by Cu^{2+} only, of all the transition metal cations and resulted into a turn-off sensing of the copper cation. Also, the selective sensitization of Eu^{3+} resulted in a bright red luminescence (*119*). A turn-on fluorescent sensing mechanism was reported for the sensing of Hg^{2+} in water using lanthanide MOF (Eu-isophthalate) nanoparticles. An acid-base resistant Zn-based MOF constructed from 5-aminoisophthalic acid was utilized for the luminescent sensing of Hg^{2+}. The Zn-MOF contains uncoordinated carboxylic oxygen atoms and exhibited a pronounced fluorescent and selective response to Hg^{2+} over other metals present in the solution (*120*). A 3D cadmium MOF constructed from 5-(4-pyridyl)-tetrazolate and 1,4-naphthalenedicarboxylic acid was reported for its stability under heat, acidic and

basic conditions. It was reported to be the first MOF that could selectively sense Cr^{3+} in aqueous solution by turn-on fluoresecence emission. The enhancement was as a result of the coordination of the analyte ion with oxygen and nitrogen atoms of the ligand (*84*). In another report, MIL-82 which has a carboxyl-rich group was designed as a parent MOF. In conjunction, a stable Ln-MOF was successfully developed by doping the Eu^{3+} cation on the coordination sites of MIL-82. The strong luminescence of Eu^{3+}- incorporated MIL-82 signified that the uncoordinated carboxyl group is a proficient scaffold for accommodating and sensitizing Eu^{3+} cations. This type of Lu-MOFs is a highly selective (relatively low detection limit of 0.09 mM) and effective chemical sensor for Ag^{+} in aqueous medium. This Lu-MOF has an outstanding water and thermal stability, which provided intermittent technique for detecting Ag^{+} in water samples (*71*). A Zinc-MOF of 2,6-naphthalenedicarboxylic acid was incorporated with Eu^{3+} ions via solvothermal and post-synthetic modification (PSM) techniques. Eu^{3+}@Zn-NDC exhibited three sensing channels for Cr^{3+} and three good linearities ranging from 1×10^{-3} to 7.5×10^{-5} mol/L. These parameters enhanced the sensitivity, selectivity and quantitative response of the Zn-MOF to Cr^{3+} in aqueous media (*121*). An electrochemical MOF-based sensor was reported for the detection of Pb^{2+} ions where NH_2-MIL-53(Cr) was incorporated on the surface of a glass carbon electrode (GCE). A good electronic response for Pb^{2+} was obtained as the oxidation current increased on increasing the concentration in the range 0.4-80 μm and an LOD value of 30.5 nM was obtained (*122*). Tran et al. also reported on the immobilization MIL-53(Fe), on GCE and its use for the electrochemical sensing of Cd^{2+} in water. The resulting electrode exhibited a stable electrochemical behavior and the response signal was enhanced. Therefore, it was used for the detection of Cd^{2+} using the differential pulse voltammetry technique and the LOD was reported to be 16 nM (*123*). The first recyclable MOF for the detection of phosphate anion was constructed from Eu and 1,3,5-benzenetribenzoate.The anion was selectively sensed in the presence of other anions. The luminescence intensity remained intact after five sensing cycles. This indicates a weak interaction between the MOF and phosphate anion (*124*). NH_2-functionalized terephthalic acid linker was employed in the synthesis of NH_2-MIL-53(Al) used for the detection of free ClO^{-} ions. The fluorescence of the MOF material was quenched on exposure to the free chlorine. The LOD and detection range were 0.04 μm and 0.05 – 15 μm respectively. The quenching was attributed to energy transfer through the hydrogen bond interaction between the ClO^{-} ions and the amino group of the MOF framework (*125*). In another report, CN^{-} anion was selectively sensed by post-synthetic modified ZIF-90 which incorporated specific active sites with the cyanide anion over some other anions. The LOD obtained met the WHO (World Health Organization) standard for the permissible limits of CN^{-} concentration in drinking water (*126*). A MOF hybrid, Cu-MOF/rGO was fabricated and electrode-modified for the electrochemical detection of nitrite anion. This sensor gave an LOD value of 33 nm and distinguishable selectivity for nitrite anion over interfering ions (*127*). Xia et al. reported the fluorescence quenching of a Cd(II)-MOF for the sensing of $Cr_2O_7^{2-}$ anion in water. The quenching was more on increasing the concentration of the anion, showing that the extent of quenching depended on the concentration of the analyte. The detection was as a result of the competition absorption and energy transfer mechanism (*128*). Also for the selective detection of $Cr_2O_7^{2-}$, a Zn-MOF was encapsulated with proflavin dye. The dye-encapsulated MOF exhibited green emission which was selectively quenched by the anion even in the presence of other competing anions. Fe^{3+} cation was also selectively detected

by the same MOF material. The fluorescence quenching was attributed to light absorption by the analyte and the quenching mechanism was found to be static (*129*).

There are also reports on the detection of toxic organic pollutants. Yang et al. reported the electrochemical sensing of three co-existing dihydroxybenzene (DBI) isomers, namely catechol (CT), resorcinol (RS) and hydroquinone (HQ). Chitosan and rGO were coated on the surface of an electrode, resulting into a high electrical conductivity. In this composite was grafted an electroactive MOF, $Cu_3(BTC)_2$ (Figure 3). There were intense voltametric signals of the analytes at the electrode as a result of the porous framework of $Cu_3(BTC)_2$ and the electronic conductive composite. Quantitative analysis showed the LOD for the analytes were 0.44, 0.41 and 0.33 μm for HQ, CT and RS respectively. Satisfactory results were obtained in the use of the developed sensor for real water sample (*130*). $Cu_3(BTC)_2$-modified on carbon paste electrode was also used for the electrochemical detection studies of 2,4-dichlorophenol using cyclic voltammetry and differential pulse voltammetry. The sensor was also used for the analyte sensing in reservoir raw water samples. The sensor exhibited good selectivity toward the analyte, LOD of 9 nM and wide linear range detection within 0.04 – 1.0 μm (*131*). Further on DBI detection, Ni@graphene composites were obtained from a thermally-annealed Ni-BTC MOF. A sensor for the detection of HQ and CT was fabricated using the composite and glassy carbon electrode. Both DBIs could not be differentiated using the bare electrode, as only one oxidation peak was found from cyclic voltammetry measurements. Two distinct peaks were seen with the use of the composite and GCE, this indicated that both DBIs could be differentiated. In addition, the sensor was binder-free and easy to prepare (*132*). Two La(III)-based MOFs of 5-aminoisophthalic and oxalic acids were synthesized and found to display high sensitivity in the selective detection of acetone over several other analytes like acetonitrile, dimethylformamide, dimethylsulfoxide, ethyl acetate, etc. This was achieved by fluorescence quenching as a result of the interaction between the framework and acetone. Initially, there was reduction in the fluorescent emission intensity and eventually, there was full quenching (*133*). A Zn-MOF synthesized using 1,3,5-tris(3-carboxy-triazolemethylene)-2,4,6-tritoluene (H_3L) as organic ligand, produced a potential fluorescent material that could selectively and sensitively detectnitrobenzene in aqueous solution (*134*). In another report, a dual-functional Co(II) MOF was reported for its low detection limit of 14 and 4 μm for acetylacetone and Hg^{2+} by fluorescence emission quenching. The quenching was attributed to the resonance energy transfer from the excited Co-MOF to the analytes. The good recyclability of the MOF material was also reported (*135*). Li et al. reported on a yttrium-MOF of 2,5-furandicarboxylate for the selective recognition and luminescence sensing of Cu^{2+}, nitrobenzene and o-chlorophenol with LOD values of 0.1 μg/ml, 5 and 10 mg/L respectively. The fluorescence intensity was found to decrease on increasing the analytes concentration. The study presented a highly selective MOF for the detection of metal ions and small organic molecules (*136*).

Sensing of PPCPs is necessary due to their ubiquitous and hazardous nature when present in waterbodies in large quantities. The sensing of tetracycline (an antibiotic) using a stable luminescent Zr-MOF was documented. Results of the theoretical and experimental studies were in close consonance, the mechanism being fluorescence quenching attributed to the transfer of photo-induced electron from the organic ligand to tetracycline. Furthermore, the efficiency of the analyte sensing was enhanced by pre-concentrating the analyte in the pores of the MOF framework (*137*). A Zn-based MOF, NUC-6 (NUC-North University of China), was discovered to be luminescent and multi-responsive as it could detect both nitrofuran antibiotics (nitrofurazone and nitrofurantoin) and dichloronitroaniline pesticide in water by the quenching of its luminescence intensity. It exhibited

detection limits of 116, 16 and 12 ppb for dichloronitroaniline, nitrofurantoin and nitrofurazone respectively. Optical spectroscopy and quantum chemical calculation inferred that the mechanism of sensing by luminescent quenching was dominated by internal filter effect and photo-induced electron transfer (*138*).

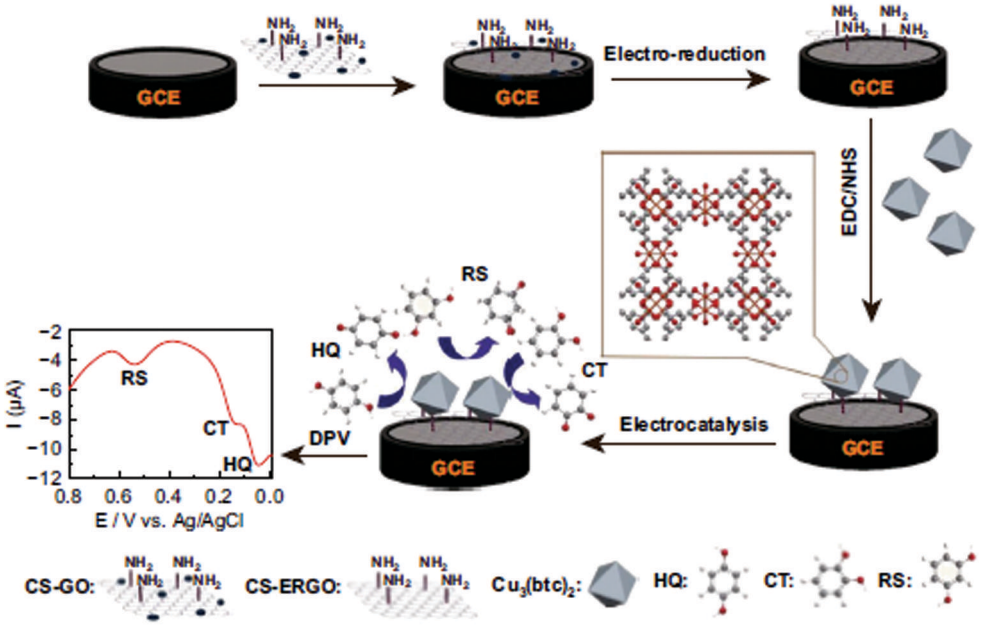

Figure 3. Detection of catechol (CT), resorcinol (RS), and hydroquinone (HQ) with MOF $Cu_3(BTC)_2$ and CS/rGO composite. Reproduced with permission from reference (130). Copyright 2016 American Chemical Society.

4. Environmental Applications of MOF-Based Materials for Adsorption of Pollutants

Adsorptive removal of toxic pollutants, either in gaseous state or from aqueous solution, is preferred to other techniques for remediation. This is because it is less energy intensive, relatively cheap, simple to operate, produces low harmful secondary products and could be carried out at low temperature. Furthermore, the adsorbent materials could be recycled (*45*). The selection of an ideal adsorbent is paramount to ensure the effectiveness of an adsorption operation. The adsorbent must possess high porosity and large surface area (*139*). MOFs are well known for their high surface area and high porosity. More interestingly, they are capable of selective adsorption of target species due to the presence of functionalities in their structure as shown in Figure 4. These functionalities could confer a profound impact on the adsorption efficiency through increased interaction between the functionalities and the adsorbates (*1*). These interactions are acid-base, electrostatic, coordination, hydrogen bonding, π-π, etc. (*140*) Electrostatic interactions are the commonest of these interactions. These are based on the surface charges of the material depending on the level of acidity or basicity of the medium. It could also be achieved when some particular species are present (*141*).

Consequently, electrostatic interaction could occur between the charged compound and oppositely charged adsorbates. π-π stacking interactions occur when aromatic rings are present in the structures of both the MOF and adsorbate (*142*). Hydrogen bonding is another important interaction for adsorption process. It is formed between two electrovalent atoms (N, O, F) where one

withdraws electrons from hydrogen atom involved in a covalent bond and the other possesses a lone pair of electrons (*143*). Acid-base interaction also contributes to adsorption mechanisms in which Lewis bases could coordinate to CUS of MOFs (*144*).

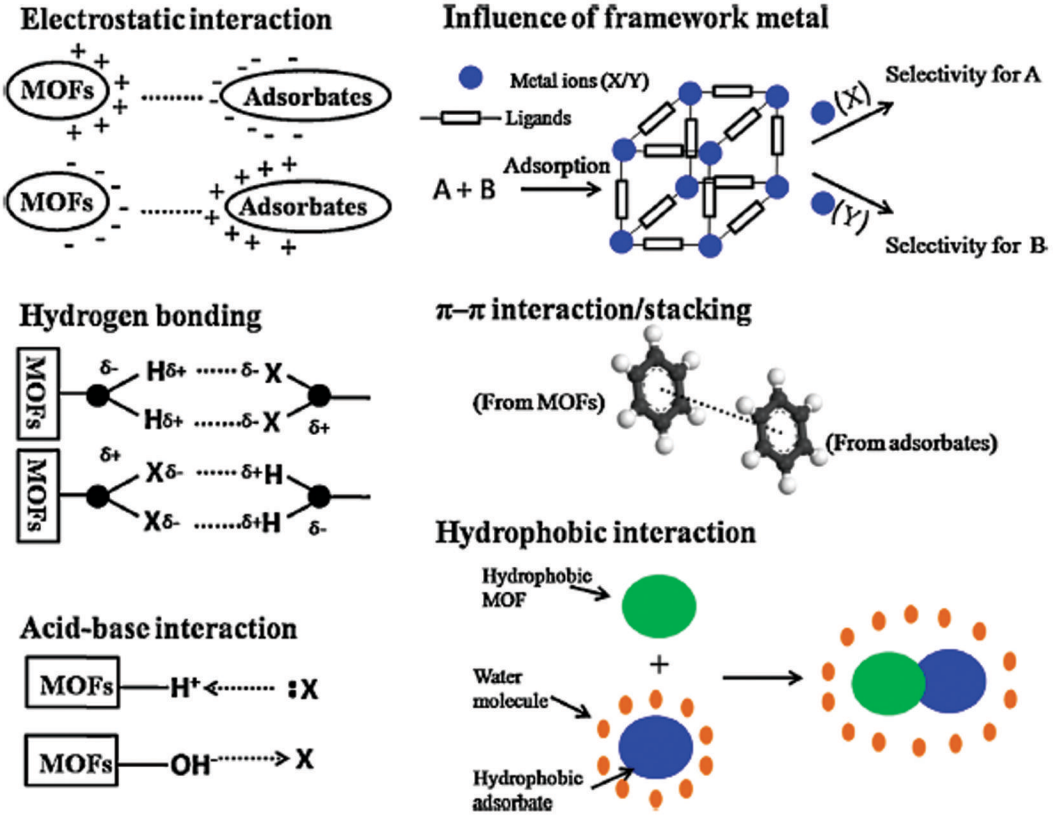

Figure 4. Possible adsorptive removal mechanisms of hazardous materials over MOFs. Reproduced with permission from reference (*140*). *Copyright 2015 Elsevier.*

However, as discussed earlier, there are new advances in the modification of MOFs to make them more effective in their use as adsorbents. For the functionalized MOFs, the introduced groups on the pristine MOFs could further interact with target adsorbate through different mechanisms (e.g., electrostatic, acid-base, hydrogen bonding, etc.), thus leading to better adsorption efficiency than the pristine form. MOF materials could also be composited with suitable materials for the enhancement of their adsorptive capability based on the synergy of the adsorptive efficiency of the compositing materials. The porosity of the MOFs is enhanced, this invariably gives rise to better adsorption performance. The functionalities of the MOF materials are tuned by the incorporation of the compositing materials, and in most cases, new properties that are desirable for adsorption processes are conferred on the MOF structure (*45*). Such materials include metal oxides, metal nanoparticles, graphene oxide, etc. (*145–147*) Another class of MOF-based materials are the MOF-derived carbons, also known as MOF derivatives. These are derived when MOF materials are pyrolyzed. They offer benefits like ordered structure, higher surface area, porosity, chemical stability and therefore higher adsorptive efficiency than the pristine MOFs (*148*).

In the subsequent section, the application of MOF-based materials in the adsorption of both gaseous and water pollutants would be discussed. Figure 5 illustrates some contaminants adsorbed using MOF-based materials.

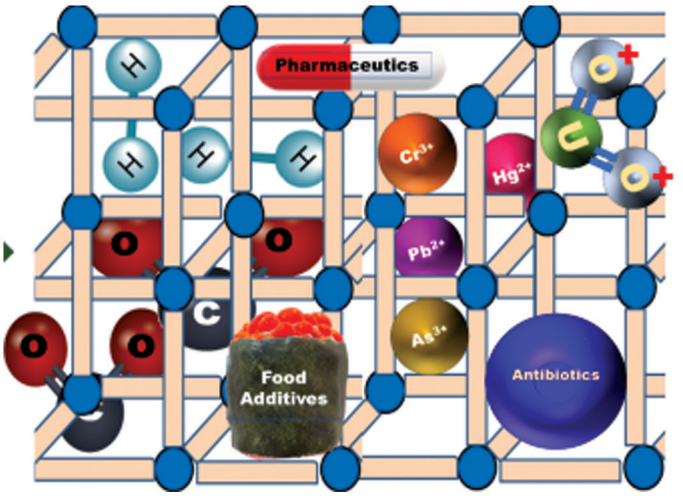

Figure 5. Application of MOF-based derivatives for adsorption of contaminants. Reproduced with permission from reference (*149*). *Copyright 2020 Elsevier.*

4.1. MOF-Based Materials for Adsorption of Gaseous Pollutants

MOFs have received a substantial application, in the removal of toxic air pollutants from flue gases due to their large surface areas, high porosity, pore tunability and distinct interactions (*150*). For the adsorption of CO_2, MOF-177 and MOF-5 are among the most studied MOFs and have been applied in real life scenarios. Particularly, MOF-177 with the brand name Basolite® Z377, have been commercialized (*151*). MOF-177 and MOF-5 were investigated for CO_2 adsorption and compared to 5A zeolite (traditional adsorbent). The adsorption capacity was found to be greater than that of 5A zeolite with high pressures in consideration. However, 5A zeolite has high affinity for CO_2 at sub-atmospheric pressure. MOF-177 displayed a fair CO_2/NO_2 selectivity and good regeneration capacity. Also, the potential of Cu-BTC MOF for CO_2 adsorption was investigated. The MOF was impregnated with 1-butyl-3-methylimidazolium acetate which doubled the adsorption capacity of CO_2 in comparison to pristine MOF at 15 kPa. The functionalized MOF was regenerated after many CO_2 desorption cycles (*152*). Cu-BTC was also impregnated with lithium nitrate, and was heat-treated under vacuum. The adsorption capacity of the impregnated MOF doubled that of the pristine MOF. Also, the adsorption process was completely reversible. This was attributed to the overlap of the CO_2 equilibrium adsorption and desorption curve of the lithium doped Cu-BTC MOF (*153*). A magnesium variant of MOF-74 (Mg-CPO-27) was also investigated for the adsorption of CO_2 and it exhibited an outstanding adsorption capacity under ambient temperature. Also, the regenerating capacity was studied and the CO_2 adsorption and desorption branches of isotherms were found to overlap (*154*). Recently, Edubilli et al. investigated a litmus test on UiO-66 MOF. This was carried

out by packing a column with MOF constituting a combined pressure vacuum swing adsorption. The purity of CO_2 obtained and adsorption capacity were close to values obtained with other MOFs (*155*).

Gate opening phenomena is one of the attracting functions of flexible MOFs, during an adsorption process. This process is applicable to MOFs with no pores or even small pores, such that when introduced to certain gas molecules, the pores would expand. This expansion is directly dependent on the interaction of the MOF with the surface of the adsorbate (Figure 6). ZIF-20 has a 3D structure, which includes large cages connected through small windows. The selective adsorption of CO_2 over methane, at 760 torr and 273 K was five times greater. This was attributed to stronger connection between the pore surface and CO_2 molecules. The gas molecules were able to pass through the framework due to the process of window widening. Moreover, the flexibility of ZIF-20 framework was impacted by the exertion of quadrupole moment of CO_2 (*156*).

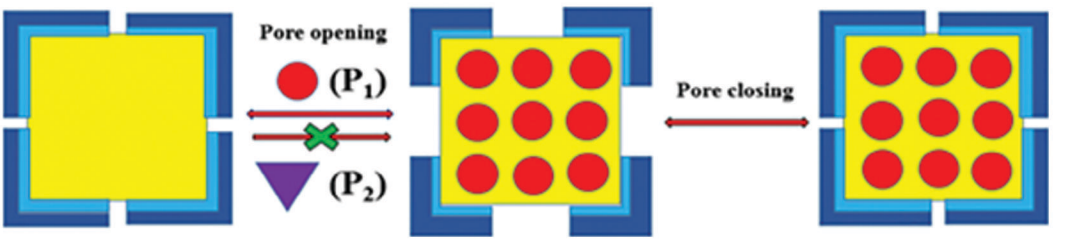

Figure 6. Schematic representation of selective gas adsorption in a flexible MOF centered on gate opening phenomena and specific pressure guests. Red circles and purple triangle represent sorbable and non-sorbable guest molecules. Reproduced with permission from reference (*156*). *Copyright 2020 Elsevier.*

Carbon monoxide is mainly produced from partial oxidation of compounds containing carbon, in a mixture constituting CO_2, N_2, hydrocarbons and H_2. The removal of carbon mononoxide (CO) is mainly carried by coordinating unsaturated metals with CO (*83*). Considering the capacity, MOF-74 is a very effective MOF, in which the adsorption strength could be attuned by changing the metals. CO-metal binding in Cu(aip)(H_2O) (aip = 5-azidoisophthalate), could lead to a deformation in the structure, which further improves the adsorption of CO. Also, a combination of spin-state transition and CO-metal binding in Fe-BTTri (H_3BTTri= 1,3,5-tris (1H-1,2,3-triazol-5-yl) benzene) have also been employed for CO removal. ZIF-8 was doped onto Au/TiO_2 for the oxidation of CO (*157*). A series of M-MOF-74 (where M= Mn^{2+}, Zn^{2+} Mg^{2+}, Fe^{2+}, Ni^{2+}, Co^{2+}), were investigated on CO adsorption. The CO-, Ni- and Fe-MOF-74 displayed an outstanding adsorption capacity at 1.2 bar and 298 K (*158*).

Table 1 shows the adsorption capacities of some MOF-based materials for CO_2 and other gases.

Table 1. Different Gas Adsorption Capacities of Selected MOFs

MOFs	*Adsorbate*	*Removal (mol/kg)*	*Operating conditions (Temperature/Pressure)*	*Reference*
ZIF-8	CO_2	9.10	303 K/4500 kPa	(*159*)
PCN-250(Fe_3)	CO_2	5.24	303 K	(*160*)
		3.02	298 K/100 kPa	(*161*)
UiO-66	CO_2	4.34	298 K/2000 kPa	(*162*)
Li-doped UiO-66	CO_2	2.80	298 K/100 kPa	(*163*)
MOF-177	CO_2	1.00	298 K/100 kPa	(*164*)
Cu-BTC	CO_2	11.70	297 K/1500 kPa	(*165*)
Ionic liquid-Functionalized MOF-177	CO_2	1.70	303 K/100 kPa	(*166*)
Tetraethylenepentamine-Funtionalized Mg-MOF-74	CO_2	6.11	298 K/100 kPa	(*167*)
Ionic liquid-Functionalized Cu-BTC	CO_2	1.70	303 K/15 kPa	(*152*)
MOF-177	SO_2	25.70	293 K/100 kPa	(*168*)
UiO-66	NO_2	1.59	298 K	(*169*)
Ba-doped Cu-BTC	SO_2	2.71	773 K	(*170*)
Cu-BTC		0.71		
Al-fumarate	DCM	3.40	298 K/44.70 kPa	(*171*)
	TCM	2.52	298 K/21.44 kPa	
UiO-66	Toluene	1.64	298 K	(*172*)
MOF-177	ethylbenzene	2.13	298 K/0.39 kPa	
	Ethenylbenzene Benzene	1.61	298 K/0.23 kPa	
	Toluene	8.82	298 K/4.88 kPa	(*173*)
	acetone	3.77	298 K/1.44 kPa	
		8.30	298 K/10.83 kPa	

Notes: DCM – dichloromethane; TCM – trichloromethane

Sulfur dioxide (SO_2) is a dominant oxide of sulfur, emitted in the environment via combustion of sulfur-containing fuels. SO_2 reacts with water to form acid rain which can have lethal effect on environmental health (*174*) HKUST-1 has been investigated for the removal of tetrahydrothiophene and thiophene. 78 wt% was achieved for sulfur removal from model oils containing thiophene. Conjugated polycarbazole porous MOFs ortho-Cz-POF, para-Cz-POF and meta-Cz-POF have been utilized in the removal of 3-methylthiophene (*175*). During adsorption process, MOFs interact with sulfur compounds available in the fuel through π-π coordination sites which have selected metal ions such as Cu^+, Ni^{2+}, Zn^{2+}, Cu^{2+} and Co^{2+}, hence, the effectiveness of the following MOFs: UMCM-152, CuCl/MIL-47(V), MIL-101(Cr), MIL-100(Fe), MOF-505, PWA/HKUST-1 and HKUST-1 (*174*). Functionalized and pristine UiO-66(Zr) have been tested for the adsorption of benzothiophene and thiophene. The modification was carried out by introducing an amino group on the linker and the introduction of carboxylic group at the defective site. HKUST-1, composited with graphene oxide (GO/HKUST-1) has also been reported as an effective adsorbent. The adsorption capacity was found to be 60.67 mg S/g, and was attributed to the improvement in the porosity with composite formation (*176*). Three different MOFs [MIL-160, MOF-177 and amine-functionalized MIL-125(Ti))] were investigated for SO_2 adsorption. MOF-177 shows a potential for industrial applications in a short-medium period with an adsorption capacity of 25.70 mol/kg (293 K). The adsorption isotherm was Type V, which indicated low affinity between the adsorbent and the adsorbate (*168*).

Ammonia (NH_3) gas can strongly bind to unsaturated metal sites and prevent recycling of materials (*177*, *178*). NH_3 removal has been investigated by utilizing robust MOFs with unsaturated metal sites such as M_2Cl_2(BTDD)-$(H_2O)_2$ (M = Mn, Co, Ni, H_2BTDD = 1*H*-1,2,3-triazolo[4,5-b],[4′,5′-i])dibenzo-[1,4]dioxin). The MOF showed high uptake (15.47 mmol/g) at 1 bar and 298 K as reported (*179*). Some of the other routes involve interaction between MOF functional groups (such as hydroxyl, ammonium and sulfonic) and NH_3. The importance of functional groups on the removal of NH_3 has been investigated by using Grand Canonical Monte Carlo simulations applied to a database of 137,953 hypothetical MOFs (*180*). Zr-based MOFs such as UiO-66$(OH)_2$, UiO-66OH, UiO-66, UiO-66-$(COOH)_2$ and UiO-66-NO_2 have also been investigated for the removal of NH_3. The presence of different functional groups such as -COOH, -NO_2, -SO_3H and NH_2 has greatly improved the adsorption of NH_3 under humid and dry conditions (*181*). Ammonia is a Bronsted base with high affinity for sulfonic and carboxylic acids. Hence, presence of such functional groups on MOFs could act as strong capture sites for ammonia. UiO-66-NH_2 was modified with anhydrous HCl. In comparison to pristine MOF, the UiO-66-NH_3Cl produced showed high uptake for ammonia in low pressure regions and at ambient temperature (*182*).

Hydrogen sulfide (H_2S) is an invisible gas that possesses an offensive odor. H_2S converts to a more stable product (sulfuric acid), in the atmosphere, thereby posing a threat to aquatic life and vegetation. The removal of H_2S was investigated using MIL-101(Cr)-SO_3Ag. The adsorption capacity was 96.75 mg/g with a very good cyclic stability. The H_2S adsorption was due to the interaction between Ag and S (*183*). The use of different functionalized UiO-66(Zr)-XN materials for H_2S removal by molecular investigation have been investigated. UiO-66-(Zr)-$(COOH)_2$ showed more activity (*184*). MIL-68(Al) was investigated using both theoretical and experimental approaches (high pressure of about 12 bar) for H_2S removal. A conclusion was made based on the

obtained result, that the triangular pores of the MOF were partially filled by some solvent molecules, due to incomplete material activation (*185*). HKUST-1/GO and HKUST-1 have also been studied for H_2S removal. As a result of unsaturated copper sites in the structure of the MOF, both reactive and physical adsorption took place. Also, the stability of both materials, in the presence of water led to gradual degradation, indicating chemisorption (*186*). Pristine and functionalized UiO-66(Zr) were investigated in removing H_2S from binary gas mixtures. UiO-66-COOH and UiO-66$(COOH)_2$ showed the highest capacity, in comparison to other tested solids. This may be due to high isosteric heat of adsorption. This suggests an interaction between the polar H_2S molecules and the hydrophilic groups, which favors the adsorption process (*187*, *188*). From a stability standpoint, ZIF-8 has also shown a promising activity for H_2S removal (*189*, *190*).

A major class of air pollutants is VOCs with a potential for mutagenesis, carcinogenesis and tetratogenesis. These characteristics are capable of endangering human health and ecological environment (*191*). VOCs emission of anthropogenic nature arises from different industrial operations which include petroleum refining, natural gas and crude oil exploration (*192*). The potential of Cu-BTC MOF was investigated on fourteen VOCs and semi-VOCs. The adsorption capacity was higher than displayed by three non-MOF adsorbents (*193*). Al-fumarate MOF has also been tested for the adsorption of dichloromethane and trichloromethane (DCM and TCM respectively). The evaluated adsorption capacity was high for DCM and DCM/TCM selectivity. The phenomenon was attributed to differences in adsorbent molecule size. The small DCM molecules could easily have contact with the pores of the Al-fumarate and take advantage of the active site than that of DCM (*171*). The adsorption of toluene on UiO-66 was also investigated. The presence of moisture contributed negatively to the toluene adsorption capacity. This was an indication of competition in the adsorption process between water vapor and toluene. The reusability study was favorable under thermal treatment, after three cycles (*9*).

Fluorinated compounds such as chlorofluorocarbons (CFCs) belong to a class of gaseous pollutants, considered harmful to the atmosphere. In the last decades, there has been a gradual substitution with other service fluid types in place of CFCs, in refrigeration processes. This practice has helped in significant recovery of the functionality of the planetary ultraviolet shield (*191*). MOF-177 was investigated for the adsorption of sevoflurane (SF), the adsorbent showed high affinity and the adsorption efficiency was impressive. However, the presence of moisture observed in the vent line of the breathing system, challenged its implementation as an anesthetic scavenger (*194*). MIL-101 displayed a higher SF/H_2O selectivity with the packed column experiment in comparison to the conventional adsorbent, which suffers the effects of "roll-up" when saturation was attained by the test column. MIL-101 showed high stability after several desorption cycles (*195*).

4.2. MOF-Based Materials for Adsorption of Water Pollutants

MOF materials have been studied for water purification. These studies have proved the efficiency of MOFs for this intent. Their effectiveness is due of their high surface area, tunable porosity, controlled pore size, possibility of the modification of their structure, among others. Table 2 shows the adsorption capacities of some examples of MOF-based materials for the adsorption of water pollutants

For the adsorptive removal of heavy metals, a stable anionic MOF, AMOF-1 of 5,5′-(1,4-phenylenebis(methylene))bis(oxy) diisophthalic acid was developed and subsequently used to capture heavy metal ions Pb(II), Cd(II) and Hg(II) at ppm level. 98.7% removal of Hg(II) was

attained after 24 hours. The adsorption capacities were 71, 41 and 78 mg/g respectively. The adsorption capacity was attributed to metal inclusion into the MOF structure by cation exchange (*196*). As a result of the affinity of sulfur atom to some metals, sulfur-containing functionalities are incorporated onto MOF structures. According to the hard/soft acid/base (HSAB) theory by Pearson (*197*), sulfur atom could interact with metal atoms and form chelates with them, thereby aiding their adsorption from aqueous solution. Example is the use of 2,2′-dithiodibenzoic acid for the synthesis of a zirconium MOF. This MOF was capable of selective removal of Au ions from water (*198*). NENU-400 (Northeast Normal University-400) contains free-standing thioether groups. It was prepared and employed for the adsorptive removal of Hg^{2+} and was found effective due to the interaction between the thioether group and the Hg^{2+} (*199*). The already modified NH_2-UiO-66 could still be further modified with other functionalities using several reagents which are linked by the exposed amino group (*200*). NH_2-UiO-66 was modified with DMTD (dimercapto-1,3,4-thiadiazole) for the introduction of hydrogen sulfide which enhanced the removal of Hg^{2+} (*201*). Other reagents like resorcyl aldehyde (RSA)and thioctic acid which were meant to increase the numbers of –OH groups, were used to modify UiO-66 for the removal of Pb(II) and Au(III) respectively (*201*, *202*). Carboxylic (-COOH), sulfonic ($–SO_3H$), nitro ($-NO_2$), etc. are other functional groups that have been reported to be incorporated into MOF structures, and gave better performance than pristine MOFs (*203*, *204*). The magnetic property of iron-based materials, useful for the separation of adsorbents from the adsorption medium after use, has motivated their use as composite materials (*205*). A magnetic MOF functionalized with CTAB and a MOF (Fe_3O_4@UiO-66@UiO-67) were used to remove Cr(VI) from water. UiO-66 served as the core and UiO-67 as the shell. Outstanding removal capacity was obtained and Fe_3O_4 was useful in separating the MOF composite from the adsorption medium after the removal process. Very high adsorption capacity of 932.1 mg/g obtained was due to tunable pores, surface active sites and electrostatic interactions. The composite showed a remarkable adsorption capacity in a wide pH range of 1.0–11.0 (*206*). Graphene oxide (GO), when incorporated into MOFs, confers enhanced adsorption capacity and water stability to the resulting MOF composite. Lu et al. reported the hydrothermal synthesis of MIL-101(Fe)/GO in which a sandwich structure was formed with the MOF distributed uniformly on the graphene oxide sheet. Its use for the adsorption of Pb^{2+} was reported (*146*). Chitosan was incorporated into UiO-66 and was found to have an adsorption capacity of 94 mg/g for Cr(VI). Its higher capacity than chitosan could be attributed to the electrostatic interaction between the amino group or the oxygen atom of the linker and the metal ions (*207*).

For the removal of pharmaceuticals and personal care products(PPCPs), adsorptive uptake of phenol and p-nitrophenol (PNP) from water on MIL-100 (Fe and Cr) and NH_2-MIL-101-Al) was studied (*208*). The latter showed a better adsorption capacity, as a result of H-bonding interaction between nitrophenol and the $–NH_2$ groups on the compound. A study reported the adsorption of amodiaquine, an antimalarial, from water. The zinc CPs used were $[Zn_2(fum)_2(bpy)]$ (fum - fumarate; bpy - 4,4-bipyridine) and $[Zn_4O\ (bdc)_3]$ (bdc-1,4-benzenedicarboxylate). The highest adsorption capacity was achieved within three hours with adsorption capacity of 0.478 mg/g on $[Zn_2(fum)_2(bpy)]$ and 47.62 mg/g on $[Zn_4O(bdc)_3]$ at pH of 4.3 (*209*). A 3D MOF $\{[Cu_2(L).(H_2O)_2]$(L=2,5-bis(3′,5′-dicarboxylphenyl)-benzoic acid) was used for the adsorption of chlorpromazine hydrochloride and diclofenac sodium. The adsorption of the latter was faster than the former. There was a weak interaction between the drugs and the $–COO^-$ groups of the MOF.

The result presented an effective adsorbent for both pharmaceuticals (*204*). Several functionalities, capable of producing these interactions, have been introduced onto the MOF structure either by PSM or direct synthesis using already functionalized ligands (*210*). Hydroxyl group (-OH) introduced onto MOF structures could act as hydrogen bond donor or acceptor, and therefore bring about hydrogen-bonding interaction with the adsorbate. MIL-101(Cr)–OH and MIL-101(Cr)–$(OH)_3$ were prepared using ethanolamine or triethanolamine as reagents to supply the –OH groups, for the adsorption of some PPCPs namely, bisphenol A, triclosan, naproxen, etc. These –OH groups were noted to interact with oxygen atoms in the PPCPs, in a hydrogen donor-acceptor interaction (*211*). The adsorption efficiency was found to increase with an increase in the number of –OH groups in the MOFs. A decrease in the porosity of MIL-101 after functionalization with –OH group was observed. Despite this, there was an increased adsorptive uptake of the PPCPs adsorbed compared to pure MIL-101. This was also as a result of the hydrogen bond between the adsorbent and oxygen atoms of the adsorbate (*212*). In addition to the H-bonding interaction observed for the –OH functional group, amino (-NH_2) functional group could undergo electrostatic interaction with the target adsorbate. Lv et al. reported MIL-68(Ln)–NH_2 for p-Arsanilic acid adsorption. The high adsorptive removal was attributed to hydrogen bonding, electrostatic and π-π interaction between the functionalities of the adsorbate and the organic ligand (*213*). Although, this functionalization processes reduced the porosity of the pristine MOF, higher adsorptive removal was obtained due to the greater interaction between the adsorbate and the introduced functionalities on the MOF structure. The removal of diclofenac was achieved on CTAB-ZIF-67. Enhanced result (compared to CTAB-free ZIF-67) was obtained due to the electrostatic interaction caused by the positive surface charge of the functionalized MOF (*214*). The first ever synthesized MOF-5 which has a surface area 151 m^2/g, was carbonized and gave a porous carbon of surface area 1731 m^2/g. Higher adsorption capacities for bisphenol A, sulfamethoxazole and methyl orange dye than commercial activated carbon were reported. The excellent performance was attributed to the much higher surface area, preserved morphology, unique meso/macropore structure, cooperative interaction of a pore-filling mechanism, hydrogen bonding and electrostatic interaction (*215*). PPCPs, ibuprofen and diclofenac were adsorbed using pyrolyzed ZIF-8. The pyrolysis was done at different temperature ranging from 800-1200°C. It was noted that several functional groups like phenolic, lactonic and carboxylic groups served as hydrogen bond donors for interaction with the acceptors of the PPCPs (*216*). Another investigation on the use of MOF-derived carbon for the adsorption of PPCPs, atenolol and clofibric acid was carried out. An adsorption capacity of 552 and 540 mg/g respectively, was displayed and electrostatic interaction contributed to this. A simple solvent washing method regenerated the spent adsorbent (*217*).

For the adsorption of methylene blue and malachite green dyes, Fe_3O_4@AMCA-MIL53(Al) nanocomposite was prepared. Several chemical interactions namely hydrogen, pi-pi, electrostatic aided the adsorption process (*218*). Activated carbon is a widely used adsorbent, but its incorporation into MOFs has been explored. For instance, Hasanzadeh et al. reported its incorporation into MIL-101 (Cr) for the removal of direct red and acid blue. The composite was found to have higher surface area and pore volume than the individual materials. A large percentage of the dyes were removed within five minutes (*219*). Torad et al. pyrolyzed ZIF-67, made cobalt nanoparticle of the resulting nanoporous carbon and used same for the removal of methylene blue dye. An interesting observation was that the pristine MOF retained its original morphology even after pyrolysis. An outstanding adsorption capacity of 500 mg/g was obtained (*220*).

Table 2. Adsorption Capacities of Some Examples of MOF-Based Materials for the Adsorption of Water Pollutants

MOF	*Added functionality/ compositing material*	*Adsorbate*	*Adsorption capacity (mg/g)*	*Mode of interaction with adsorbate*	*Reference*
		Functionalized MOFs			
MIL-101	-OH	Naproxen	156	Hydrogen bonding	(*211*)
		Ketoprofen	80		
		Triclosan	112		
		bisphenol A	97		
		p-Chloro-m-xylenol	79		
MIL-68 (Ln)	$-NH_2$	p-Arsanilic acid	401	Electrostatic, hydrogen bonding, pi-pi	(*213*)
ZIF-67	CTAB	Diclofena (*211*)	61	Electrostatic interaction	(*80*)
UiO-66-NH_2	-SH	Hg^{2+}	670.5	Complexation reaction	(*19*)
		MOF composites			
MIL53(Al)	Fe_3O_4@AMCA	Methylene blue, malachite green	1.02 mmol/g 0.9	Hydrogen bonding, pi-pi and electrostatic interaction	(*218*)
CuMOF	Fe_3O_4	Malachite green	219	High surface area	(*221*)
		Pb^{2+}	114		
MIL-101 (Cr)	Activated carbon	Direct red acid blue	High surface area	(*219*)	
UiO-66	Chitosan	Cr(VI)	94	Electrostatic interaction	(*207*)
		MOF-derived Porous carbon			
Pyrolyzed ZIF-67	Co nanoparticles	Methylene blue	500	High surface area	(*220*)
MOF-5		Sulfamethoxazole, bisphenol A, methyl orange	625, 757 872	High surface area, preserved morphology	(*215*)
ZIF-8		Ibuprofen	320	Hydrogen bonding	(*216*)
		diclofenac	400		

5. Conclusions and Future Prospects

This chapter has revealed the potentiality of MOFs for environmental applications. Specifically, the usage of MOF-based materials for the detection and adsorption of gaseous and water pollutants have been discussed. Recent advances for the enhancement of the efficiency of MOFs include the incorporation of additional functionalities, development of MOF composites and pyrolysis of MOFs to obtain carbon materials. For sensing applications, conductive materials have been introduced into MOFs for better electrochemical sensing of analytes. These strategies have proven effective in achieving better results with MOFs for environmental applications.

Despite the fascinating results that have been achieved, there are still some challenges to be addressed as far as the environmental application of MOFs is concerned.

Firstly, the scalability of the materials is imperative. It is worthwhile to scale-up the synthesis of the materials for industrial use. Likewise, it is required that the scaled-up samples retain the properties possessed when prepared in laboratory scale. Secondly, studies on the application of these materials for real life scenarios are still scarce. Similarly, the performances of MOF-based adsorbents in real solutions containing mixed adsorbates, presence of salts or humic acids and in low concentration of contaminants should be investigated for commercial applications. Thirdly, the water stability of MOFs must be considered irrespective of the sensing/adsorption performance. In view of this, additional research is needed to develop MOF materials with better water stability. Fourthly, theoretical studies on process optimization and the interactions between the analytes and MOF materials should be embarked on for the design of MOF-based sensors and adsorbents. In addition, there is an urgent need to explore MOF-based adsorbents for purification applications not only for water and air, but for fuel-based contaminants. Lastly, studies focusing on the detection and removal of new contaminants are also essential to determine the potential of MOFs application in removing emerging contaminants / pollutants. Overall, this chapter has revealed that MOFs, with or without modifications, have great potentials in detecting and removing air and water pollutants.

Acknowledgments

Authors appreciate Landmark University, Nigeria, for the use of facilities to carry out this project.

References

1. Yoo, D. K.; Bhadra, B. N.; Jhung, S. H. Adsorptive Removal of Hazardous Organics from Water and Fuel with Functionalized Metal-Organic Frameworks: Contribution of Functional Groups. *J. Hazard. Mater* **2021**, *403* (August 2020), 123655. https://doi.org/10.1016/j.jhazmat.2020.123655.
2. Jang, S.; Song, S.; Lim, J. H.; Kim, H. S.; Phan, B. T.; Ha, K. T.; Park, S.; Park, K. H. Application of Various Metal-Organic Frameworks (Mofs) as Catalysts for Air and Water Pollution Environmental Remediation. *Catalysts* **2020**, *10* (2), 1–32. https://doi.org/10.3390/catal10020195.
3. Fang, X.; Zong, B.; Mao, S. Metal–Organic Framework-Based Sensors for Environmental Contaminant Sensing. *Nano-Micro Lett* **2018**, *10* (4), 1–19. https://doi.org/10.1007/s40820-018-0218-0.

4. Zhang, Y.; Yuan, S.; Feng, X.; Li, H.; Zhou, J.; Wang, B. Preparation of Nanofibrous Metal-Organic Framework Filters for Efficient Air Pollution Control. *J. Am. Chem. Soc* **2016**, *138* (18), 5785–5788. https://doi.org/10.1021/jacs.6b02553.
5. Islamoglu, T.; Chen, Z.; Wasson, M. C.; Buru, C. T.; Kirlikovali, K. O.; Afrin, U.; Mian, M. R.; Farha, O. K. Metal-Organic Frameworks against Toxic Chemicals. *Chem. Rev.* **2020**, *120* (16), 8130–8160. https://doi.org/10.1021/acs.chemrev.9b00828.
6. Li, P.; Li, J.; Feng, X.; Li, J.; Hao, Y.; Zhang, J.; Wang, H.; Yin, A.; Zhou, J.; Ma, X.; Wang, B. Metal-Organic Frameworks with Photocatalytic Bactericidal Activity for Integrated Air Cleaning. *Nat. Commun.* **2019**, *10* (1), 1–10. https://doi.org/10.1038/s41467-019-10218-9.
7. Nie, J.; Xie, H.; Zhang, M.; Liang, J.; Nie, S.; Han, W. Effective and Facile Fabrication of MOFs/Cellulose Composite Paper for Air Hazards Removal by Virtue of in Situ Synthesis of MOFs/Chitosan Hydrogel. *Carbohydr. Polym.* **2020**, *250* (February), 12125–12128. https://doi.org/10.1016/j.carbpol.2020.116955.
8. Liang, C. S.; Duan, F. K.; He, K. Bin; Ma, Y. L. Review on Recent Progress in Observations, Source Identifications and Countermeasures of PM2.5. *Environ. Int.* **2016**, *86*, 150–170. https://doi.org/10.1016/j.envint.2015.10.016.
9. Zhang, Q.; Li, Q.; Young, T. M.; Harper, D. P.; Wang, S. A Novel Method for Fabricating an Electrospun Poly(Vinyl Alcohol)/Cellulose Nanocrystals Composite Nanofibrous Filter with Low Air Resistance for High-Efficiency Filtration of Particulate Matter. *ACS Sustain. Chem. Eng.* **2019**, *7* (9), 8706–8714. https://doi.org/10.1021/acssuschemeng.9b00605.
10. Zhang, P.; Huang, Y.; Rao, Y.; Chen, M.; Li, X.; Ho, W.; Lee, S.; Cao, J. Chemical Etching Fabrication of Uniform Mesoporous Bi@Bi2O3 Nanospheres with Enhanced Visible Light-Induced Photocatalytic Oxidation Performance for NOx. *Chem. Eng. J.* **2021**, *406* (August 2020), 126910. https://doi.org/10.1016/j.cej.2020.126910.
11. Srivastava, R. K.; Jozewicz, W.; Singer, C. SO2 Scrubbing Technologies: A Review. *Environ. Prog.* **2001**, *20* (4), 219–228. https://doi.org/10.1002/ep.670200410.
12. Ryu, H. J.; Grace, J. R.; Lim, C. J. Simultaneous CO2/SO2 Capture Characteristics of Three Limestones in a Fluidized-Bed Reactor. *Energy and Fuels* **2006**, *20* (4), 1621–1628. https://doi.org/10.1021/ef050277q.
13. Li, J.; Han, X.; Zhang, X.; Sheveleva, A. M.; Cheng, Y.; Tuna, F.; McInnes, E. J. L.; McCormick McPherson, L. J.; Teat, S. J.; Daemen, L. L.; Ramirez-Cuesta, A. J.; Schröder, M.; Yang, S. Capture of Nitrogen Dioxide and Conversion to Nitric Acid in a Porous Metal–Organic Framework. *Nat. Chem.* **2019**, *11* (12), 1085–1090. https://doi.org/10.1038/s41557-019-0356-0.
14. Vikrant, K.; Tsang, D. C. W.; Raza, N.; Giri, B. S.; Kukkar, D.; Kim, K. H. Potential Utility of Metal-Organic Framework-Based Platform for Sensing Pesticides. *ACS Appl. Mater. Interfaces* **2018**, *10* (10), 8797–8817. https://doi.org/10.1021/acsami.8b00664.
15. Iranpour, R.; Stenstrom, M.; Tchobanoglous, G.; Miller, D.; Wright, J.; Vossoughi, M. Environmental Engineering: Energy Value of Replacing Waste Disposal with Resource Recovery. *Science (80-.)* **1999**, *285* (5428), 706–711. https://doi.org/10.1126/science.285.5428.706.
16. Saeed, T.; Naeem, A.; Ud Din, I.; Alotaibi, M. A.; Alharthi, A. I.; Wali Khan, I.; Huma Khan, N.; Malik, T. Structure, Nomenclature and Viable Synthesis of Micro/Nanoscale Metal

Organic Frameworks and Their Remarkable Applications in Adsorption of Organic Pollutants. *Microchem. J.* **2020**, *159*, 105579. https://doi.org/10.1016/j.microc.2020.105579.
17. Jain, S. N.; Shaikh, Z.; Mane, V. S.; Vishnoi, S.; Mawal, V. N.; Patel, O. R.; Bhandari, P. S.; Gaikwad, M. S. Nonlinear Regression Approach for Acid Dye Remediation Using Activated Adsorbent: Kinetic, Isotherm, Thermodynamic and Reusability Studies. *Microchem. J.* **2019**, *148* (May), 605–615. https://doi.org/10.1016/j.microc.2019.05.024.
18. Li, Y.; Hu, T.; Chen, R.; Xiang, R.; Wang, Q.; Zeng, Y.; He, C. Novel Thiol-Functionalized Covalent Organic Framework as Adsorbent for Simultaneous Removal of BTEX and Mercury (II) from Water. *Chem. Eng. J.* **2020**, *398* (April), 125566. https://doi.org/10.1016/j.cej.2020.125566.
19. Fu, L.; Wang, S.; Lin, G.; Zhang, L.; Liu, Q.; Fang, J.; Wei, C.; Liu, G. Post-Functionalization of UiO-66-NH2 by 2,5-Dimercapto-1,3,4-Thiadiazole for the High Efficient Removal of Hg(II) in Water. *J. Hazard. Mater.* **2019**, *368* (January), 42–51. https://doi.org/10.1016/j.jhazmat.2019.01.025.
20. Li, J.; Wang, X. X.; Zhao, G.; Chen, C.; Chai, Z.; Alsaedi, A.; Hayat, T.; Wang, X. X. Metal-Organic Framework-Based Materials: Superior Adsorbents for the Capture of Toxic and Radioactive Metal Ions. *Chem. Soc. Rev.* **2018**, *47* (7), 2322–2356. https://doi.org/10.1039/c7cs00543a.
21. Yi, X. H.; Wang, F. X.; Du, X. D.; Fu, H.; Wang, C. C. Highly Efficient Photocatalytic Cr(VI) Reduction and Organic Pollutants Degradation of Two New Bifunctional 2D Cd/Co-Based MOFs. *Polyhedron* **2018**, *152*, 216–224. https://doi.org/10.1016/j.poly.2018.06.041.
22. Abazari, R.; Reza Mahjoub, A.; Slawin, A. M. Z.; Carpenter-Warren, C. L. Morphology- and Size-Controlled Synthesis of a Metal-Organic Framework under Ultrasound Irradiation: An Efficient Carrier for PH Responsive Release of Anti-Cancer Drugs and Their Applicability for Adsorption of Amoxicillin from Aqueous Solution. *Ultrason. Sonochem.* **2018**, *42*, 594–608. https://doi.org/10.1016/j.ultsonch.2017.12.032.
23. Chi, H.; Wan, J.; Ma, Y.; Wang, Y.; Ding, S.; Li, X. Ferrous Metal-Organic Frameworks with Stronger Coordinatively Unsaturated Metal Sites for Persulfate Activation to Effectively Degrade Dibutyl Phthalate in Wastewater. *J. Hazard. Mater.* **2019**, *377* (May), 163–171. https://doi.org/10.1016/j.jhazmat.2019.05.081.
24. Jiang, J.; Yaghi, O. M. Brønsted Acidity in Metal − Organic Frameworks. *Chem. Rev.* **2015**, *115*, 6966–6997. https://doi.org/10.1021/acs.chemrev.5b00221.
25. Tranchemontagne, D. J.; Mendoza-Cortes, J. L.; O'Keeffe, M.; Yaghi, O. M. Secondary Building Units, Nets and Bonding in the Chemistry of Metal-Organic Frameworks. *Chem Soc Rev* **2009**, *38*, 1257.
26. Yaghi, O. M.; Li, G.; Li, H. Selective Binding and Removal of Guests in a Microporous Metal–Organic Framework. *Nature* **1995**, *378* (6558), 703–706. https://doi.org/10.1038/378703a0.
27. Lu, W.; Wei, Z.; Gu, Z. Y.; Liu, T.-F.; Park, J.; Park, J.; Tian, J. M.; Zhang, Q. Z.; Thomas, G.; Mathieu, B.; Hong-Cai, Z. Tuning the Structure and Function of Metal–Organic Frameworks via Linker Design. *Chem. Soc. Rev.* **2014**, *43*, 5561–5593.
28. Nagarkar, S. S.; Joarder, B.; Chaudhari, A. K.; Mukherjee, S.; Ghosh, S. K. Highly Selective Detection of Nitro Explosives by a Luminescent Metal-Organic Framework. *Angew. Chemie - Int. Ed.* **2013**, *52* (10), 2881–2885. https://doi.org/10.1002/anie.201208885.

29. Tran, T. Van; Cao, V. D.; Nguyen, V. H.; Hoang, B. N.; Vo, D. V. N.; Nguyen, T. D.; Bach, L. G. MIL-53 (Fe) Derived Magnetic Porous Carbon as a Robust Adsorbent for the Removal of Phenolic Compounds under the Optimized Conditions. *J. Environ. Chem. Eng.* **2020**, *8* (1), 102902. https://doi.org/10.1016/j.jece.2019.102902.
30. Yap, M. H.; Fow, K. L.; Chen, G. Z. Synthesis and Applications of MOF-Derived Porous Nanostructures. *Green Energy Environ.* **2017**, *2* (3), 218–245. https://doi.org/10.1016/j.gee.2017.05.003.
31. Yaghi, O. M.; O'Keeffe, M.; Ockwig, N. W.; Chae, H. K.; Eddaoudi, M.; Kim, J. Reticular Synthesis and the Design of New Materials. *Nature* **2003**, *423* (6941), 705–714. https://doi.org/10.1038/nature01650.
32. Evans, J. D.; Sumby, C. J.; Doonan, C. J. Post-Synthetic Metalation of Metal-Organic Frameworks. *Chem. Soc. Rev.* **2014**, *43*, 5933–5951.
33. Juan-Alcañiz, J.; Gascon, J.; Kapteijn, F. Metal-Organic Frameworks as Scaffolds for the Encapsulation of Active Species: State of the Art and Future Perspectives. *J. Mater. Chem.* **2012**, *22* (20), 10102–10119. https://doi.org/10.1039/c2jm15563j.
34. Kitagawa, S.; Kitaura, R.; Noro, S. I. Functional Porous Coordination Polymers. *Angew. Chemie - Int. Ed.* **2004**, *43* (18), 2334–2375. https://doi.org/10.1002/anie.200300610.
35. Murray, L. J.; Dincˇa, M.; Long, J. R. Hydrogen Storage in Metal-Organic Frameworks. *Chem. Soc. Rev.* **2009**, *38*, 1294–1314.
36. Van De Voorde, B.; Bueken, B.; Denayer, J.; De Vos, D. Adsorptive Separation on Metal-Organic Frameworks in the Liquid Phase. *Chem. Soc. Rev.* **2014**, *43* (16), 5766–5788. https://doi.org/10.1039/c4cs00006d.
37. Tan, H.; Ma, C.; Gao, L.; Li, Q.; Song, Y.; Xu, F.; Wang, T.; Wang, L. Metal-Organic Framework-Derived Copper Nanoparticle@carbon Nanocomposites as Peroxidase Mimics for Colorimetric Sensing of Ascorbic Acid. *Chem. - A Eur. J.* **2014**, *20* (49), 16377–16383. https://doi.org/10.1002/chem.201404960.
38. Wang, H.; Zhu, Q. L.; Zou, R.; Xu, Q. Metal-Organic Frameworks for Energy Applications. *Chem* **2017**, *2* (1), 52–80. https://doi.org/10.1016/j.chempr.2016.12.002.
39. Zhang, X.; Li, G.; Wu, D.; Li, X.; Hu, N.; Chen, J.; Chen, G.; Wu, Y. Recent Progress in the Design Fabrication of Metal-Organic Frameworks-Based Nanozymes and Their Applications to Sensing and Cancer Therapy. *Biosens. Bioelectron.* **2019**, *137* (May), 178–198. https://doi.org/10.1016/j.bios.2019.04.061.
40. Jiao, L.; Seow, J. Y. R.; Skinner, W. S.; Wang, Z. U.; Jiang, H. L. Metal–Organic Frameworks: Structures and Functional Applications. *Mater. Today* **2019**, *27* (August), 43–68. https://doi.org/10.1016/j.mattod.2018.10.038.
41. Hu, Y. H.; Zhang, L. Hydrogen Storage in Metal-Organic Frameworks. *Adv. Mater.* **2010**, *22* (20), 117–130. https://doi.org/10.1002/adma.200902096.
42. Li, Y.; Gai, T.; Lin, Y.; Zhang, W.; Li, K.; Liu, Y.; Duan, Y.; Li, B.; Ding, J.; Li, J. Eight Cd(II) Coordination Polymers with Persistent Room-Temperature Phosphorescence: Intriguing Dual Emission and Time-Resolved Afterglow Modulation. *Inorg. Chem. Front.* **2020**, 7 (3), 777–785. https://doi.org/10.1039/c9qi01273g.
43. Chen, Y. Z.; Zhang, R.; Jiao, L.; Jiang, H. L. Metal–Organic Framework-Derived Porous Materials for Catalysis. *Coord. Chem. Rev.* **2018**, *362*, 1–23. https://doi.org/10.1016/j.ccr.2018.02.008.

44. Cui, Y.; Li, B.; He, H.; Zhou, W.; Chen, B.; Qian, G. Metal-Organic Frameworks as Platforms for Functional Materials. *Acc. Chem. Res.* **2016**, *49* (3), 483–493. https://doi.org/10.1021/acs.accounts.5b00530.
45. Ahmed, I.; Jhung, S. H. Composites of Metal-Organic Frameworks: Preparation and Application in Adsorption. *Mater. Today* **2014**, *17* (3), 136–146. https://doi.org/10.1016/j.mattod.2014.03.002.
46. Liu, L.; Tai, X.; Zhou, X. Au3+/Au0 Supported on Chromium(III) Terephthalate Metal Organic Framework (MIL-101) as an Efficient Heterogeneous Catalystfor Three-Component Coupling Synthesis of Propargylamines. *Materials (Basel)* **2017**, *10* (2) https://doi.org/10.3390/ma10020099.
47. Qiu, Q.; Chen, H.; Wang, Y.; Ying, Y. Recent Advances in the Rational Synthesis and Sensing Applications of Metal-Organic Framework Biocomposites. *Coord. Chem. Rev.* **2019**, *387*, 60–78. https://doi.org/10.1016/j.ccr.2019.02.009.
48. Carne, A.; Carbonell, C.; Imaz, I.; Maspoch, D. Nanoscale Metal–Organic Materials. *Chem Soc Rev* **2011**, *40*, 291–305.
49. Jiang, D.; Chen, M.; Wang, H.; Zeng, G.; Huang, D.; Cheng, M.; Liu, Y.; Xue, W.; Wang, Z. W. The Application of Different Typological and Structural MOFs-Based Materials for the Dyes Adsorption. *Coord. Chem. Rev.* **2019**, *380*, 471–483. https://doi.org/10.1016/j.ccr.2018.11.002.
50. Rehman, A.; Farrukh, S.; Hussain, A.; Pervaiz, E. Synthesis and Effect of Metal–Organic Frame Works on CO2 Adsorption Capacity at Various Pressures: A Contemplating Review. *Energy Environ.* **2020**, *31* (3), 367–388. https://doi.org/10.1177/0958305X19865352.
51. Li, B.; Chrzanowski, M.; Zhang, Y.; Ma, S. Applications of Metal-Organic Frameworks Featuring Multi-Functional Sites. *Coord. Chem. Rev.* **2016**, *307*, 106–129. https://doi.org/10.1016/j.ccr.2015.05.005.
52. Mu, F.; Dai, B.; Zhao, W.; Zhang, L.; Xu, J.; Guo, X. A Review on Metal-Organic Frameworks for Photoelectrocatalytic Applications. *Chinese Chem. Lett.* **2020**, *31* (7), 1773–1781. https://doi.org/10.1016/j.cclet.2019.12.015.
53. Zheng, X.; Wang, L.; Liu, M.; Lei, P.; Liu, F.; Xie, Z. Nanoscale Mixed-Component Metal-Organic Frameworks with Photosensitizer Spatial-Arrangement-Dependent Photochemistry for Multimodal-Imaging-Guided Photothermal Therapy. *Chem. Mater.* **2018**, *30* (19), 6867–6876. https://doi.org/10.1021/acs.chemmater.8b03043.
54. Falcaro, P.; Hill, A. J.; Nairn, K. M.; Jasieniak, J.; Mardel, J. I.; Bastow, T. J.; Mayo, S. C.; Gimona, M.; Gomez, D.; Whitfield, H. J.; Riccò, R.; Patelli, A.; Marmiroli, B.; Amenitsch, H.; Colson, T.; Villanova, L.; Buso, D. A New Method to Position and Functionalize Metal-Organic Framework Crystals. *Nat. Commun.* **2011**, *2* (1), 237. https://doi.org/10.1038/ncomms1234.
55. Ricco, R.; Malfatti, L.; Takahashi, M.; Hill, A. J.; Falcaro, P. Applications of Magnetic Metal-Organic Framework Composites. *J. Mater. Chem. A* **2013**, *1* (42), 13033–13045. https://doi.org/10.1039/c3ta13140h.
56. Huang, D.; Wang, G.; Cheng, M.; Zhang, G.; Chen, S.; Liu, Y.; Li, Z.; Xue, W.; Lei, L.; Xiao, R. Optimal Preparation of Catalytic Metal-Organic Framework Derivatives and Their Efficient Application in Advanced Oxidation Processes. *Chem. Eng. J.* **2021**, *421* (November), 127817. https://doi.org/10.1016/j.cej.2020.127817.

57. Chen, X.; Peng, X.; Jiang, L.; Yuan, X.; Yu, H.; Wang, H.; Zhang, J.; Xia, Q. Recent Advances in Titanium Metal–Organic Frameworks and Their Derived Materials: Features, Fabrication, and Photocatalytic Applications. *Chem. Eng. J.* **2020**, *395* (April), 125080. https://doi.org/10.1016/j.cej.2020.125080.
58. Lykourinou, V.; Chen, Y.; Wang, X. Sen; Meng, L.; Hoang, T.; Ming, L. J.; Musselman, R. L.; Ma, S. Immobilization of MP-11 into a Mesoporous Metal-Organic Framework, MP-11@mesoMOF: A New Platform for Enzymatic Catalysis. *J. Am. Chem. Soc.* **2011**, *133* (27), 10382–10385. https://doi.org/10.1021/ja2038003.
59. Li, Z.; Zeng, H. C. Surface and Bulk Integrations of Single-Layered Au or Ag Nanoparticles onto Designated Crystal Planes {110} or {100} of ZIF-8. *Chem. Mater.* **2013**, *25* (9), 1761–1768. https://doi.org/10.1021/cm400260g.
60. Bradshaw, D.; Garai, A.; Huo, J. Metal–Organic Framework Growth at Functional Interfaces: Thin Films and Composites for Diverse Applications. *Chem. Soc. Rev.* **2012**, *41* (6), 2344–2381. https://doi.org/10.1039/c1cs15276a.
61. Uemura, T.; Yanai, N.; Kitagawa, S. Polymerization Reactions in Porous Coordination Polymers. *Chem. Soc. Rev.* **2009**, *38* (5), 1228–1236. https://doi.org/10.1039/b802583p.
62. Li, X.; Zhu, Q.-L. L. MOF-Based Materials for Photo- and Electrocatalytic CO2 Reduction. *EnergyChem* **2020**, *2* (3), 100033. https://doi.org/10.1016/j.enchem.2020.100033.
63. Zhang, W.; Hu, Y.; Ge, J.; Jiang, H. L.; Yu, S. H. A Facile and General Coating Approach to Moisture/Water-Resistant Metal-Organic Frameworks with Intact Porosity. *J. Am. Chem. Soc.* **2014**, *136* (49), 16978–16981. https://doi.org/10.1021/ja509960n.
64. Lee, K. J.; Lee, J. H.; Jeoung, S.; Moon, H. R. Transformation of Metal-Organic Frameworks/Coordination Polymers into Functional Nanostructured Materials: Experimental Approaches Based on Mechanistic Insights. *Acc. Chem. Res.* **2017**, *50* (11), 2684–2692. https://doi.org/10.1021/acs.accounts.7b00259.
65. Cao, X.; Tan, C.; Sindoro, M.; Zhang, H. Hybrid Micro-/Nano-Structures Derived from Metal-Organic Frameworks: Preparation and Applications in Energy Storage and Conversion. *Chem. Soc. Rev.* **2017**, *46* (10), 2660–2677. https://doi.org/10.1039/c6cs00426a.
66. Zhai, M.; Wang, F.; Du, H. Transition-Metal Phosphide-Carbon Nanosheet Composites Derived from Two-Dimensional Metal-Organic Frameworks for Highly Efficient Electrocatalytic Water-Splitting. *ACS Appl. Mater. Interfaces* **2017**, *9* (46), 40171–40179. https://doi.org/10.1021/acsami.7b10680.
67. Liu, H.; Ma, Y.; Chen, J.; Wen, M.; Li, G.; An, T. Highly Efficient Visible-Light-Driven Photocatalytic Degradation of VOCs by CO2-Assisted Synthesized Mesoporous Carbon Confined Mixed-Phase TiO2 Nanocomposites Derived from MOFs. *Appl. Catal. B Environ.* **2019**, *250* (February), 337–346. https://doi.org/10.1016/j.apcatb.2019.03.054.
68. Song, Y.; Cho, D.; Venkateswarlu, S.; Yoon, M. Systematic Study on Preparation of Copper Nanoparticle Embedded Porous Carbon by Carbonization of Metal-Organic Framework for Enzymatic Glucose Sensor. *RSC Adv.* **2017**, *7* (17), 10592–10600. https://doi.org/10.1039/c7ra00115k.
69. Dong, W.; Zhuang, Y.; Li, S.; Zhang, X.; Chai, H.; Huang, Y. High Peroxidase-like Activity of Metallic Cobalt Nanoparticles Encapsulated in Metal–Organic Frameworks Derived Carbon for Biosensing. *Sensors Actuators, B Chem.* **2018**, *255*, 2050–2057. https://doi.org/10.1016/j.snb.2017.09.013.

70. Chen, Y.; Zhang, R.; Jiao, L.; Jiang, H. Metal – Organic Framework-Derived Porous Materials for Catalysis. *Coord. Chem. Rev.* **2018**, *362*, 1–23. https://doi.org/10.1016/j.ccr.2018.02.008.
71. Ge, K. M.; Wang, D.; Xu, Z. J.; Chu, R. Q. A Luminescent Eu(III)-MOF for Selective Sensing of Ag+ in Aqueous Solution. *J. Mol. Struct.* **2020**, *1208*, 127862. https://doi.org/10.1016/j.molstruc.2020.127862.
72. Wang, X. F.; Song, X. Z.; Sun, K. M.; Cheng, L.; Ma, W. MOFs-Derived Porous Nanomaterials for Gas Sensing. *Polyhedron* **2018**, *152*, 155–163. https://doi.org/10.1016/j.poly.2018.06.037.
73. Lin, L. C.; Kim, J.; Kong, X.; Scott, E.; McDonald, T. M.; Long, J. R.; Al., E. Understanding CO2 Dynamics in Metal– Organic Frameworks with Open Metal Sites. *Angew Chem Int Ed* **2013**, *125* (16), 4506–4509.
74. Zhang, J. P.; Zhang, Y. B.; Lin, J. Bin; Chen, X. M. Metal Azolate Frameworks: From Crystal Engineering to Functional Materials. *Chem. Rev.* **2012**, *112* (2), 1001–1033. https://doi.org/10.1021/cr200139g.
75. Lei, J.; Qian, R.; Ling, P.; Cui, L.; Ju, H. Design and Sensing Applications of Metal – Organic Framework Composites. *Trends Anal. Chem.* **2014**, *58*, 71–73. https://doi.org/10.1016/j.trac.2014.02.012.
76. Kreno, L. E.; Leong, K.; Farha, O. K.; Allendorf, M.; Van Duyne, R. P.; Hupp, J. T. Metal–Organic Framework Materials as Chemical Sensors. *Chem. Rev.* **2012**, *112* (2), 1105–1125. https://doi.org/10.1021/cr200324t.
77. Li, W.; Wu, X.; Han, N.; Chen, J.; Tang, W.; Chen, Y. Core-Shell Au@ZnO Nanoparticles Derived from Au@MOF and Their Sub-Ppm Level Acetone Gas-Sensing Performance. *Powder Technol.* **2016**, *304*, 241–247.
78. Cui, Y.; Zhang, J.; He, H.; Qian, G. Photonic Functional Metal-Organic Frameworks. *Chem. Soc. Rev.* **2018**, *47* (15), 5740–5785. https://doi.org/10.1039/c7cs00879a.
79. Liu, F.; Gao, W.; Li, P.; Zhang, X. M.; Liu, J. P. Lanthanide Metal-Organic Frameworks as Multifunctional Luminescent Sensor for Detecting Cations, Anions and Organic Solvent Molecules in Aqueous Solution. *J. Solid State Chem.* **2017**, *253*, 202–210. https://doi.org/10.1016/j.jssc.2017.05.040.
80. Lin, X. M.; Niu, J. L.; Lin, J.; Hu, L.; Zhang, G.; Cai, Y. P. A Luminescent Tb(III)-MOF Based on Pyridine-3, 5-Dicarboxylic Acid for Detection of Nitroaromatic Explosives. *Inorg. Chem. Commun.* **2016**, *72*, 69–72. https://doi.org/10.1016/j.inoche.2016.08.009.
81. Gładysiak, A.; Nguyen, T. N.; Navarro, J. A. R.; Rosseinsky, M. J.; Stylianou, K. C. A Recyclable Metal–Organic Framework as a Dual Detector and Adsorbent for Ammonia. *Chem. - A Eur. J.* **2017**, *23* (55), 13602–13606. https://doi.org/10.1002/chem.201703510.
82. Li, H. Y.; Zhao, S. N.; Zang, S. Q.; Li, J. Functional Metal-Organic Frameworks as Effective Sensors of Gases and Volatile Compounds. *Chem. Soc. Rev.* **2020**, *49* (17), 6364–6401. https://doi.org/10.1039/c9cs00778d.
83. Li, H.; Wang, K.; Sun, Y.; Lollar, C. T.; Li, J.; Zhou, H. C. Recent Advances in Gas Storage and Separation Using Metal–Organic Frameworks. *Mater. Today* **2018**, *21* (2), 108–121. https://doi.org/10.1016/j.mattod.2017.07.006.

84. Li, H.; Li, D.; Qin, B.; Li, W.; Zheng, H.; Zhang, X. Turn-on Fluorescence in a Stable Cd (II) Metal-Organic Framework for Highly Sensitive Detection of Cr3+ in Water. *Dye. Pigment.* **2020**, *178*, 108359. https://doi.org/10.1016/j.dyepig.2020.108359.
85. Homayoonnia, S.; Zeinali, S. Design and Fabrication of Capacitive Nanosensor Based on MOF Nanoparticles as Sensing Layer for VOCs Detection. *Sensors Actuators, B Chem.* **2016**, *237*, 776–786. https://doi.org/10.1016/j.snb.2016.06.152.
86. Hosseini, M. S.; Zeinali, S.; Sheikhi, M. H. Fabrication of Capacitive Sensor Based on Cu-BTC (MOF-199) Nanoporous Film for Detection of Ethanol and Methanol Vapors. *Sensors Actuators, B Chem.* **2016**, *230*, 9–16. https://doi.org/10.1016/j.snb.2016.02.008.
87. Li, W.; Wu, X.; Han, N.; Chen, J.; Qian, X.; Deng, Y.; Tang, W.; Chen, Y. MOF-Derived Hierarchical Hollow ZnO Nanocages with Enhanced Low-Concentration VOCs Gas-Sensing Performance. *Sensors Actuators, B Chem.* **2016**, *225*, 158–166. https://doi.org/10.1016/j.snb.2015.11.034.
88. Sachdeva, S.; Koper, S. J. H.; Sabetghadam, A.; Soccol, D.; Gravesteijn, D. J.; Kapteijn, F.; Sudhölter, E. J. R.; Gascon, J.; De Smet, L. C. P. M. Gas Phase Sensing of Alcohols by Metal Organic Framework-Polymer Composite Materials. *ACS Appl. Mater. Interfaces* **2017**, *9* (29), 24926–24935. https://doi.org/10.1021/acsami.7b02630.
89. Ghanbarian, M.; Zeinali, S.; Mostafavi, A. A Novel MIL-53(Cr-Fe)/Ag/CNT Nanocomposite Based Resistive Sensor for Sensing of Volatile Organic Compounds. *Sensors Actuators, B Chem.* **2018**, *267*, 381–391. https://doi.org/10.1016/j.snb.2018.02.138.
90. Patah, A.; Kasim, W.; Yuliarto, B. Potential Application Zn-MOF / MnO2 Composite as Methanol Gas Sensor. *Key Eng. Mater.* **2019**, *811*, 113–119. https://doi.org/10.4028/www.scientific.net/KEM.811.113.
91. Lee, J.-H.; Nguyen, T. T. T.; Nguyen, L. H. T.; Phan, T. B.; Kim, S. S.; Doan, T. L. H. Functionalization of Zirconium-Based Metal–Organic Frameworks for Gas Sensing Applications. *J. Hazard. Mater* **2020**, *403*, 124104.
92. Cao, E.; Guo, Z.; Song, G.; Zhang, Y.; Hao, W.; Sun, L.; Nie, Z. MOF-Derived ZnFe2O4 /(Fe-ZnO) Nanocomposites with Enhanced Acetone Sensing Performance. *Sensors Actuators B . Chem.* **2020**, *325*, 128783.
93. Torad, N. L.; Kim, J.; Kim, M.; Lim, H.; Na, J.; Alshehri, S. M.; Ahamad, T.; Yamauchi, Y.; Eguchi, M.; Ding, B.; Zhang, X. Nanoarchitectured Porous Carbons Derived from ZIFs toward Highly Sensitive and Selective QCM Sensor for Hazardous Aromatic Vapors. *J. Hazard. Mater.* **2021**, *405* (October 2020), 124248. https://doi.org/10.1016/j.jhazmat.2020.124248.
94. Gassensmith, J. J.; Kim, J. Y.; Holcroft, J. M.; Farha, O. K.; Stoddart, J. F.; Hupp, J. T.; Jeong, N. C. A Metal–Organic Framework-Based Material for Electrochemical Sensing of Carbon Dioxide. *J Am Chem Soc* **2014**, *136* (23), 8277–8282.
95. Chong, X.; Kim, K.; Ohodnicki, P. R.; Li, E.; Chang, C.; Wang, A. X. Ultrashort Near-Infrared Fiber-Optic Sensors for Carbon Dioxide Detection. *IEEE Sens. J.* **2015**, *15*, 5327–5332.
96. Pentyala, V.; Davydovskaya, P.; Ade, M.; Pohle, R.; Urban, G. Carbon Dioxide Gas Detection by Open Metal Site Metal Organic Frameworks and Surface Functionalized Metal Organic Frameworks. *Sensors Actuators B Chem* **2015**, *225*, 363–368.
97. Chocarro-Ruiz, B.; P´erez-Carvajal, J.; Avci, C.; Calvo-lozano, O.; Alonso, M. I.; Maspoch, D.; Lechuga, L. M. ACO2 Optical Sensor Based on Self-Assembled Metal – Organic

Framework Nanoparticles. *J. Mater. Chem. A* **2018**, *6*, 13171–13177. https://doi.org/10.1039/C8TA02767F.

98. Ye, B.; Gheorghe, A.; Hal, R. Van; Zevenbergen, M.; Tanase, S. CO2 Sensing under Ambient Conditions Using Metal–Organic Frameworks. **2020**, 1071–1076. https://doi.org/10.1039/d0me00004c.
99. Yang, Z.; Zhang, D.; Wang, D. Carbon Monoxide Gas Sensing Properties of Metal-Organic Frameworks-Derived Tin Dioxide Nanoparticles/Molybdenum Diselenide Nanoflowers. *Sensors Actuators, B Chem.* **2020**, *304* (August 2019), 127369. https://doi.org/10.1016/j.snb.2019.127369.
100. Li, H.; Zhu, H.; Sun, M.; Yan, Y.; Zhang, K.; Huang, D.; Wang, S. Manipulating the Surface Chemistry of Quantum Dots for Sensitive Ratiometric Fluorescence Detection of Sulfur Dioxide. *Langmuir* **2015**, *31* (31), 8667–8671. https://doi.org/10.1021/acs.langmuir.5b02340.
101. Che, S.; Dao, R.; Zhang, W.; Lv, X.; Li, H.; Wang, C. Designing an Anion-Functionalized Fluorescent Ionic Liquid as an Efficient and Reversible Turn-off Sensor for Detecting SO2. *Chem. Commun.* **2017**, *53* (27), 3862–3865. https://doi.org/10.1039/c7cc00676d.
102. Perea-Cachero, A.; Calvo, P.; Romero, E.; Téllez, C.; Coronas, J. Enhancement of Growth of MOF MIL-68(Al) Thin Films on Porous Alumina Tubes Using Different Linking Agents. *Eur. J. Inorg. Chem.* **2017**, *2017* (19), 2532–2540. https://doi.org/10.1002/ejic.201700302.
103. Chernikova, V.; Yassine, O.; Shekhah, O.; Salama, K. N. Highly Sensitive and Selective SO2 MOF Sensor: The Integration of MFM-300 MOF as a Sensitive Layer on a Capacitive Interdigitated Electrode. *J. Mater. Chem. A Mater. energy Sustain* **2018**, *6*, 5550–5554. https://doi.org/10.1039/C7TA10538J.
104. Zhang, J.; Xia, T.; Zhao, D.; Cui, Y.; Yang, Y.; Qian, G. In Situ Secondary Growth of Eu(III)-Organic Framework Film for Fluorescence Sensing of Sulfur Dioxide. *Sensors Actuators, B Chem.* **2018**, *260*, 63–69. https://doi.org/10.1016/j.snb.2017.12.187.
105. Ingle, N.; Mane, S.; Sayyad, P.; Bodkhe, G.; AL-Gahouari, T.; Mahadik, M.; Shirsat, S.; Shirsat, M. D. Sulfur Dioxide (SO2) Detection Using Composite of Nickel Benzene Carboxylic (Ni3BTC2) and OH-Functionalized Single Walled Carbon Nanotubes (OH-SWNTs). *Front. Mater.* **2020**, *7* (May), 1–7. https://doi.org/10.3389/fmats.2020.00093.
106. Zhou, L.-J.; Zhang, X.-X.; Zhang, W.-Y. Sulfur Dioxide Sensing Properties of MOF-Derived ZnFe2O4 Functionalized with Reduced Graphene Oxide at Room Temperature. *Rare Met.* **2020**, *40*, 1604–1613.
107. Li, H.; Feng, X.; Guo, Y.; Chen, D.; Li, R.; Ren, X.; Jiang, X.; Dong, Y.; Wang, B. A Malonitrile-Functionalized Metal-Organic Framework for Hydrogen Sulfide Detection and Selective Amino Acid Molecular Recognition. *Sci. Rep.* **2014**, *4* (4366), 1–5. https://doi.org/10.1038/srep04366.
108. Wan, X.; Wu, L.; Zhang, L.; Song, H.; Lv, Y. Novel Metal-Organic Frameworks-Based Hydrogen Sulfide Cataluminescence Sensors. *Sensors Actuators, B Chem.* **2015**, *220*, 614–621. https://doi.org/10.1016/j.snb.2015.05.125.
109. Yassine, O.; Shekhah, O.; Assen, A. H.; Belmabkhout, Y.; Salama, K. N.; Eddaoudi, M. H2S Sensors: Fumarate-Based Fcu-MOF Thin Film Grown on a Capacitive Interdigitated Electrode. *Angew. Chemie - Int. Ed.* **2016**, *55* (51), 15879–15883. https://doi.org/10.1002/anie.201608780.

110. Zhang, C.; Zhang, S.; Yang, Y.; Yu, H.; Dong, X. Highly Sensitive H2S Sensors Based on Metal-Organic Framework Driven γ-Fe2O3 on Reduced Graphene Oxide Composites at Room Temperature. *Sensors Actuators, B Chem.* **2020**, *325*, 128804. https://doi.org/10.1016/j.snb.2020.128804.
111. Ali, A.; Alzamly, A.; Greish, Y. E.; Bakiro, M.; Nguyen, H. L.; Mahmoud, S. T. A Highly Sensitive and Flexible Metal − Organic Framework Polymer- Based H 2 S Gas Sensor. **2021**. https://doi.org/10.1021/acsomega.1c02295.
112. Travlou, N. A.; Singh, K.; Rodríguez-Castellón, E.; Bandosz, T. J. Cu-BTC MOF-Graphene-Based Hybrid Materials as Low Concentration Ammonia Sensors. *J. Mater. Chem. A* **2015**, *3* (21), 11417–11429. https://doi.org/10.1039/c5ta01738f.
113. Sel, K.; Demirci, S.; Ozturk, O. F.; Aktas, N.; Sahiner, N. NH3 Gas Sensing Applications of Metal Organic Frameworks. *Microelectron. Eng.* **2015**, *136*, 71–76. https://doi.org/10.1016/j.mee.2015.04.035.
114. Zhang, J.; Yue, D.; Xia, T.; Cui, Y.; Yang, Y.; Qian, G. A Luminescent Metal-Organic Framework Fi Lm Fabricated on Porous Al2O3 Substrate for Sensitive Detecting Ammonia. *Microporous Mesoporous Mater* **2017**, *253*, 146–150. https://doi.org/10.1016/j.micromeso.2017.06.053.
115. Wang, D.; Liu, J.; Liu, Z. A Chemically Stable Europium Metal-Organic Framework for Bifunctional Chemical Sensor and Recyclable on – o Ff – on Vapor Response. *J. soli* **2017**, *251*, 243–247. https://doi.org/10.1016/j.jssc.2017.04.032.
116. Lee, J.; Nguyen, T.; Nguyen, D.; Kim, J. Gas Sensing Properties of Mg-Incorporated Metal – Organic Frameworks. **2019**, *74*, 1–11.
117. Gamonal, A.; Sun, C.; Mariano, A. L.; Fernandez-Bartolome, E.; Guerrero-SanVicente, E.; Vlaisavljevich, B.; Castells-Gil, J.; Marti-Gastaldo, C.; Poloni, R.; Wannemacher, R.; Cabanillas-Gonzalez, J.; Costa, J. S. Divergent Adsorption-Dependent Luminescence of Amino-Functionalized Lanthanide Metal–Organic Frameworks for Highly Sensitive NO2 Sensors. *J. Phys. Chem. Lett.* **2020**, *11* (9), 3362–3368.
118. DMello, M. E.; Sundaram, N. G.; Singh, A.; Singh, A. K.; Kalidindi, S. B. An Amine Functionalized Zirconium Metal-Organic Framework as an Effective Chemiresistive Sensor for Acidic Gases. *Chem. Commun.* **2019**, *55* (3), 349–352. https://doi.org/10.1039/C8CC06875E.
119. Bhattacharyya, S.; Chakraborty, A.; Jayaramulu, K.; Hazra, A.; Maji, T. K. A Bimodal Anionic MOF: Turn-off Sensing for CuII and Specific Sensitization of EuIII. *Chem Commun* **2014**, *50*, 13567.
120. Jiang, J.; Lu, Y.; Liu, J.; Zhou, Y.; Zhao, D.; Li, C. An Acid-Base Resistant Zn-Based Metal-Organic Framework as a Luminescent Sensor for Mercury (II). *J. Solid State Chem.* **2020**, *283*, 121153. https://doi.org/10.1016/j.jssc.2019.121153.
121. Yang, H.; Zhou, C.; Yang, Y.; Chu, Z.; Yan, W.; Nie, S.; Luo, J.; Lin, S.; Wang, Y. A New Three Sensing Channels Platform of Eu@Zn-MOF for Quantitative Detection of Cr(III). *Inorg. Chem. Commun.* **2020**, *116*, 107898. https://doi.org/10.1016/j.inoche.2020.107898.
122. Guo, H. X.; Wang, D. F.; Chen, J. H.; Weng, W.; Huang, M. Q.; Zheng, Z. S. Simple Fabrication of Flake-like NH2-MIL-53(Cr) and Its Application as an Electrochemical Sensor for the Detection of Pb2+. *Chem. Eng. J.* **2016**, *289*, 479–485.

123. Tran, H. V.; Dang, H. T. M.; Tran, L. T.; Van Tran, C.; Huynh, C. D. Metal-Organic Framework MIL-53(Fe): Synthesis, Electrochemical Characterization, and Application in Development of a Novel and Sensitive Electrochemical Sensor for Detection of Cadmium Ions in Aqueous Solutions. *Adv. Polym. Technol.* **2020**, *2020*, 1–10. https://doi.org/10.1155/2020/6279278.
124. Xu, H.; Cao, C. S.; Zhao, B. A Water-Stable Lanthanide-Organic Framework as a Recyclable Luminescent Probe for Detecting Pollutant Phosphorus Anions. *Chem Commun* **2015**, *51*, 10280–10283.
125. Lu, T.; Zhang, L. C.; Sun, M. X.; Deng, D. Y.; Su, Y. Y.; Lv, Y. Amino-Functionalized Metal–Organic Frameworks Nanoplatesbased Energy Transfer Probe for Highly Selective Fluorescence Detection of Free Chlorine. *Anal. Chem* **2016**, *88* (6), 3413–3420.
126. Karmakar, A.; Kumar, N.; Samanta, P.; Desai, A. V; Ghosh, S. K. A Post-Synthetically Modified MOF for Selective and Sensitive Aqueous-Phase Detection of Highly Toxic Cyanide Ions. **2016**, 864–868. https://doi.org/10.1002/chem.201503323.
127. Saraf, M.; Rajak, R.; Mobin, S. M. A Fascinating Multitasking Cu- MOF/RGO Hybrid for High Performance Supercapacitors and Highly Sensitive and Selective Electrochemical Nitrite Sensors. *J. Mater. Chem. A* **2016**, *4* (42), 16432–16445.
128. Xia, Y.; Wang, C.; Feng, R.; Li, K.; Chang, Z.; Bu, X. A Novel Double-Walled Cd (II) Metal – Organic Framework as Highly Selective Luminescent Sensor for Cr 2 O 2 7 Anion. *Polyhedron* **2018**, *153*, 110–114. https://doi.org/10.1016/j.poly.2018.07.001.
129. Awais, M.; Ye, J.; Wang, G.; Shi, L.; Liu, Z.; Lu, H.; Zhang, S.; Ning, G. Bifunctional Chemosensor Based on a Dye-Encapsulated Metal-Organic Framework for Highly Selective and Sensitive Detection of Cr 2 O 2 7 and Fe 3 + Ions. *Polyhedron* **2020**, *185*, 114604. https://doi.org/10.1016/j.poly.2020.114604.
130. Yang, Y.; Wang, Q.; Qiu, W.; Guo, H.; Gao, F. Covalent Immobilization of Cu3(Btc)2 at Chitosan–Electroreduced Graphene Oxide Hybrid Film and Its Application for Simultaneous Detection of Dihydroxybenzene Isomers. *J. Phys. Chem. C* **2016**, *120* (18), 9794–9803.
131. Dong, S.; Suo, G.; Li, N.; Chen, Z.; Peng, L.; Fu, Y.; Yang, Q.; Huang, T. A Simple Strategy to Fabricate High Sensitive 2,4- Dichlorophenol Electrochemical Sensor Based on Metal Organic Framework Cu3(BTC)2. *Sensors Actuators B. Chem.* **2016**, *222*, 972–979.
132. Zhou, X.; Yan, X.; Hong, Z.; Zheng, X.; Wang, F. Design of Magnetic Core–Shell Ni@graphene Composites as a Novel Electrochemical Sensing Platform. *Sensors Actuators B. Chem.* **2018**, *255*, 2959–2962.
133. Wang, J.; Si, P.; Yang, J.; Zhao, S.; Li, P.; Li, B.; Wang, S.; Lu, M.; Yu, S. La (III) -Based MOFs with 5-Aminoisophthalic Acid for Optical Detection and Degradation of Organic Molecules in Water. **2019**, *162*, 255–262. https://doi.org/10.1016/j.poly.2019.01.045.
134. Gan, Y. Le; Huang, K. R.; Li, Y. G.; Qin, D. P.; Zhang, D. M.; Zong, Z. A.; Cui, L. S. Synthesis, Structure and Fluorescent Sensing for Nitrobenzene of a Zn-Based MOF. *J. Mol. Struct.* **2021**, *1223*, 129217. https://doi.org/10.1016/j.molstruc.2020.129217.
135. Su, Y.; Qu, Y.; Fu, L.; Cui, G. An Unprecedented Binodal (4 , 6) -Connected Co (II) MOF as Dual-Responsive Luminescent Sensor for Detection of Acetylacetone and Hg 2 + Ions. *Inorg. Chem. Commun.* **2020**, *118* (April), 108013. https://doi.org/10.1016/j.inoche.2020.108013.

136. Li, D.; Wang, F.; Tian, Y.; Liu, S.; Liu, D.; Yang, B. The Selective Recognition and Luminescence Sensing Demonstrated in Yttrium - Organic Framework. *Opt. Mater. (Amst).* **2020**, *108* (September), 109757. https://doi.org/10.1016/j.optmat.2020.109757.
137. Zhou, Y.; Yang, Q.; Zhang, D.; Gan, N.; Li, Q.; Cuan, J. Detection and Removal of Antibiotic Tetracycline in Water with a Highly Stable Luminescent MOF. *Sensors Actuators B. Chem.* **2018**, *262*, 137–143.
138. Fan, L.; Wang, F. A Self-Penetrating and Chemically Stable Zinc (Ii) -Organic Framework as Multi-Responsive Chemo-Sensor to Detect Pesticide and Antibiotics in Water. **2020** (May), 1–10. https://doi.org/10.1002/aoc.5960.
139. Bhatnagar, A.; Minocha, A. K. Conventional and Non-Conventional Adsorbents for Removal of Pollutants from Water - A Review. *Indian J. Chem. Technol.* **2006**, *13* (3), 203–217.
140. Hasan, Z.; Jhung, S. H. Removal of Hazardous Organics from Water Using Metal-Organic Frameworks (MOFs): Plausible Mechanisms for Selective Adsorptions. *J. Hazard. Mater.* **2015**, *283*, 329–339. https://doi.org/10.1016/j.jhazmat.2014.09.046.
141. Adeyemo, A. A.; Adeoye, I. O.; Bello, O. S. Metalorganicframeworksasadsor- Bents Fordyeadsorption:Overview,Prospectsandfuturechallenges. *Toxicol. Environ. Chem* **2012**, *94*, 1846–1863.
142. Khan, N. A.; Jhung, S. H. Adsorptive Removal and Separation of Chemicals with Metal-Organic Frameworks: Contribution of π-Complexation. *J. Hazard. Mater.* **2017**, *325*, 198–213. https://doi.org/10.1016/j.jhazmat.2016.11.070.
143. Ahmed, I.; Jhung, S. H. Applications of Metal-Organic Frameworks in Adsorption/Separation Processes via Hydrogen Bonding Interactions. *Chem. Eng. J.* **2017**, *310*, 197–215. https://doi.org/10.1016/j.cej.2016.10.115.
144. Jun, J. W.; Tong, M.; Jung, B. K.; Hasan, Z.; Zhong, C.; Jhung, S. H. Effect of Central Metal Ions of Analogous Metal-Organic Frameworks on Adsorption of Organoarsenic Compounds from Water: Plausible Mechanism of Adsorption and Water Purification. *Chem. - A Eur. J.* **2015**, *21* (1), 347–354. https://doi.org/10.1002/chem.201404658.
145. Li, B.; Wen, H. M.; Cui, Y.; Zhou, W.; Qian, G.; Chen, B. Emerging Multifunctional Metal–Organic Framework Materials. *Adv. Mater.* **2016**, *28* (40), 8819–8860. https://doi.org/10.1002/adma.201601133.
146. Lu, M.; Li, L.; Shen, S.; Chen, D.; Han, W. Highly Efficient Removal of Pb2+ by a Sandwich Structure of Metal-Organic Framework/GO Composite with Enhanced Stability. *New J. Chem.* **2019**, *43* (2), 1032–1037. https://doi.org/10.1039/c8nj05091k.
147. Mehdinia, A.; Jahedi Vaighan, D.; Jabbari, A. Cation Exchange Superparamagnetic Al-Based Metal Organic Framework (Fe3O4/MIL-96(Al)) for High Efficient Removal of Pb(II) from Aqueous Solutions. *ACS Sustain. Chem. Eng.* **2018**, *6* (3), 3176–3186. https://doi.org/10.1021/acssuschemeng.7b03301.
148. Chaikittisilp, W.; Ariga, K.; Yamauchi, Y. A New Family of Carbon Materials: Synthesis of MOF-Derived Nanoporous Carbons and Their Promising Applications. *J. Mater. Chem. A* **2013**, *1* (1), 14–19. https://doi.org/10.1039/c2ta00278g.
149. Kumar, S.; Jain, S.; Nehra, M.; Dilbaghi, N.; Marrazza, G.; Kim, K. H. Green Synthesis of Metal–Organic Frameworks: A State-of-the-Art Review of Potential Environmental and Medical Applications. *Coord. Chem. Rev.* **2020**, *420*, 213407. https://doi.org/10.1016/j.ccr.2020.213407.

150. Bobbitt, N. S.; Mendonca, M. L.; Howarth, A. J.; Islamoglu, T.; Hupp, J. T.; Farha, O. K.; Snurr, R. Q. Metal-Organic Frameworks for the Removal of Toxic Industrial Chemicals and Chemical Warfare Agents. *Chem. Soc. Rev.* **2017**, *46* (11), 3357–3385. https://doi.org/10.1039/c7cs00108h.
151. Tsivadze, A. Y.; Aksyutin, O. E.; Ishkov, A. G.; Knyazeva, M. K.; Solovtsova, O. V; Men'shchikov, I. E.; Fomkin, A. A.; Shkolin, A. V; Khozina, E. V; Grachev, V. A. Metal-Organic Framework Structures: Adsorbents for Natural Gas Storage. *Russ. Chem. Rev.* **2019**, *88* (9), 925–978. https://doi.org/10.1070/rcr4873.
152. Mohamedali, M.; Henni, A.; Ibrahim, H. Markedly Improved CO2 Uptake Using Imidazolium-Based Ionic Liquids Confined into HKUST-1 Frameworks. *Microporous Mesoporous Mater* **2019**, *284*, 98–110. https://doi.org/10.1016/j.micromeso.2019.04.004.
153. Zhou, L.; Niu, Z.; Jin, X.; Tang, L.; Zhu, L. Effect of Lithium Doping on the Structures and CO2 Adsorption Properties of Metal-Organic Frameworks HKUST-1. *ChemistrySelect* **2018**, *3* (45), 12865–12870. https://doi.org/10.1002/slct.201803164.
154. Bao, Z.; Yu, L.; Ren, Q.; Lu, X.; Deng, S. Adsorption of CO2 and CH4 on a Magnesium-Based Metal Organic Framework. *J. Colloid Interface Sci.* **2011**, *353* (2), 549–556. https://doi.org/10.1016/j.jcis.2010.09.065.
155. Edubilli, S.; Gumma, S. A Systematic Evaluation of UiO-66 Metal Organic Framework for CO2/N2 Separation. *Sep. Purif. Technol.* **2019**, *224*, 85–94. https://doi.org/10.1016/j.seppur.2019.04.081.
156. Ghanbari, T.; Abnisa, F.; Wan Daud, W. M. A. A Review on Production of Metal Organic Frameworks (MOF) for CO2 Adsorption. *Sci. Total Environ.* **2020**, *707*, 135090. https://doi.org/10.1016/j.scitotenv.2019.135090.
157. Wen, M.; Li, G.; Liu, H.; Chen, J.; An, T.; Yamashita, H. Metal-Organic Framework-Based Nanomaterials for Adsorption and Photocatalytic Degradation of Gaseous Pollutants: Recent Progress and Challenges. *Environ. Sci. Nano* **2019**, *6* (4), 1006–1025. https://doi.org/10.1039/c8en01167b.
158. Bloch, E. D.; Hudson, M. R.; Mason, J. A.; Chavan, S.; Crocellà, V.; Howe, J. D.; Lee, K.; Dzubak, A. L.; Queen, W. L.; Zadrozny, J. M.; Geier, S. J.; Lin, L. C.; Gagliardi, L.; Smit, B.; Neaton, J. B.; Bordiga, S.; Brown, C. M.; Long, J. R. Reversible CO Binding Enables Tunable CO/H2 and CO/N2 Separations in Metal-Organic Frameworks with Exposed Divalent Metal Cations. *J. Am. Chem. Soc.* **2014**, *136* (30), 10752–10761. https://doi.org/10.1021/ja505318p.
159. Danaci, D.; Singh, R.; Xiao, P.; Webley, P. A. Assessment of ZIF Materials for CO2 Capture from High Pressure Natural Gas Streams. *Chem. Eng. J.* **2015**, *280*, 486–493. https://doi.org/10.1016/j.cej.2015.04.090.
160. Wongsakulphasatch, S.; Kiatkittipong, W.; Saupsor, J.; Chaiwiseshphol, J.; Piroonlerkgul, P.; Parasuk, V.; Assabumrungrat, S. Effect of Fe Open Metal Site in Metal-Organic Frameworks on Post-Combustion CO2 Capture Performance. *Greenh. Gases Sci. Technol.* **2017**, *7* (2), 383–394. https://doi.org/10.1002/ghg.1662.
161. Chen, Y.; Qiao, Z.; Huang, J.; Wu, H.; Xiao, J.; Xia, Q.; Xi, H.; Hu, J.; Zhou, J.; Li, Z. Unusual Moisture-Enhanced CO 2 Capture within Microporous PCN-250 Frameworks. *ACS Appl. Mater. Interfaces* **2018**, *10* (44), 38638–38647. https://doi.org/10.1021/acsami.8b14400.

162. Kim, S. N.; Lee, Y. R.; Hong, S. H.; Jang, M. S.; Ahn, W. S. Pilot-Scale Synthesis of a Zirconium-Benzenedicarboxylate UiO-66 for CO2 Adsorption and Catalysis. *Catal. Today* **2015**, *245*, 54–60. https://doi.org/10.1016/j.cattod.2014.05.041.
163. Niu, Z.; Guan, Q.; Shi, Y.; Chen, Y.; Chen, Q.; Kong, Z.; Ning, P.; Tian, S.; Miao, R. A Lithium-Modified Zirconium-Based Metal Organic Framework (UiO-66) for Efficient CO2 Adsorption. *New J. Chem.* **2018**, *42* (24), 19764–19770. https://doi.org/10.1039/c8nj04945a.
164. Ullah, S.; Bustam, M. A.; Assiri, M. A.; Al-Sehemi, A. G.; Sagir, M.; Abdul Kareem, F. A.; Elkhalifah, A. E. I.; Mukhtar, A.; Gonfa, G. Synthesis, and Characterization of Metal-Organic Frameworks -177 for Static and Dynamic Adsorption Behavior of CO2 and CH4. *Microporous Mesoporous Mater* **2019**, *288*. https://doi.org/10.1016/j.micromeso.2019.109569.
165. Kloutse, F. A.; Hourri, A.; Natarajan, S.; Benard, P.; Chahine, R. Systematic Study of the Excess and the Absolute Adsorption of N2/H2 and CO2/H2 Mixtures on Cu-BTC. *Adsorption* **2019**. https://doi.org/10.1007/s10450-019-00124-3.
166. Mohamedali, M.; Henni, A.; Ibrahim, H. Investigation of CO2 Capture Using Acetate-Based Ionic Liquids Incorporated into Exceptionally Porous Metal–Organic Frameworks. *Adsorption* **2019**, *25* (4), 675–692. https://doi.org/10.1007/s10450-019-00073-x.
167. Su, X.; Bromberg, L.; Martis, V.; Simeon, F.; Huq, A.; Hatton, T. A. Postsynthetic Functionalization of Mg-MOF-74 with Tetraethylenepentamine: Structural Characterization and Enhanced CO2 Adsorption. *ACS Appl. Mater. Interfaces* **2017**, *9* (12), 11299–11306. https://doi.org/10.1021/acsami.7b02471.
168. Brandt, P.; Nuhnen, A.; Lange, M.; Möllmer, J.; Weingart, O.; Janiak, C. Metal-Organic Frameworks with Potential Application for SO2 Separation and Flue Gas Desulfurization. *ACS Appl. Mater. Interfaces* **2019**, *11* (19), 17350–17358. https://doi.org/10.1021/acsami.9b00029.
169. Ebrahim, A. M.; Levasseur, B.; Bandosz, T. J. Interactions of NO2 with Zr-Based MOF: Effects of the Size of Organic Linkers on NO2 Adsorption at Ambient Conditions. *Langmuir* **2013**, *29* (1), 168–174. https://doi.org/10.1021/la302869m.
170. Dathe, H.; Peringer, E.; Roberts, V.; Jentys, A.; Lercher, J. A. Metal Organic Frameworks Based on Cu2+ and Benzene-1,3,5-Tricarboxylate as Host for SO2 Trapping Agents. *Comptes Rendus Chim.* **2005**, *8* (3–4), 753–763. https://doi.org/10.1016/j.crci.2004.10.018.
171. Zhou, L.; Zhang, X.; Chen, Y. Facile Synthesis of Al-Fumarate Metal–Organic Framework Nano-Flakes and Their Highly Selective Adsorption of Volatile Organic Compounds. *Mater. Lett.* **2017**, *197*, 224–227. https://doi.org/10.1016/j.matlet.2017.01.120.
172. Zhang, X.; Yang, Y.; Song, L.; Chen, J.; Yang, Y.; Wang, Y. Enhanced Adsorption Performance of Gaseous Toluene on Defective UiO-66 Metal Organic Framework: Equilibrium and Kinetic Studies. *J. Hazard. Mater.* **2019**, *365*, 597–605. https://doi.org/10.1016/j.jhazmat.2018.11.049.
173. Yang, K.; Xue, F.; Sun, Q.; Yue, R.; Lin, D. Adsorption of Volatile Organic Compounds by Metal-Organic Frameworks MOF-177. *J. Environ. Chem. Eng.* **2013**, *1* (4), 713–718. https://doi.org/10.1016/j.jece.2013.07.005.
174. Kampouraki, Z. C.; Giannakoudakis, D. A.; Nair, V.; Hosseini-Bandegharaei, A.; Colmenares, J. C.; Deliyanni, E. A. Metal Organic Frameworks as Desulfurization Adsorbents of DBT and

4,6-DMDBT from Fuels. *Molecules* **2019**, *24* (24), 1–23. https://doi.org/10.3390/molecules24244525.

175. Lin, C.; Cheng, Z.; Li, B.; Chen, T.; Zhang, W.; Chen, S.; Yang, Q.; Chang, L.; Che, G.; Ma, H. High-Efficiency Separation of Aromatic Sulfide from Liquid Hydrocarbon Fuel in Conjugated Porous Organic Framework with Polycarbazole Unit. *ACS Appl. Mater. Interfaces* **2019**, *11* (43), 40970–40979. https://doi.org/10.1021/acsami.9b15815.
176. Radwan, D. R.; Matloob, A.; Mikhail, S.; Saad, L.; Guirguis, D. Metal Organic Framework-Graphene Nano-Composites for High Adsorption Removal of DBT as Hazard Material in Liquid Fuel. *J. Hazard. Mater.* **2019**, *373*, 447–458. https://doi.org/10.1016/j.jhazmat.2019.03.098.
177. Jasuja, H.; Peterson, G. W.; Decoste, J. B.; Browe, M. A.; Walton, K. S. Evaluation of MOFs for Air Purification and Air Quality Control Applications: Ammonia Removal from Air. *Chem. Eng. Sci.* **2015**, *124*, 118–124. https://doi.org/10.1016/j.ces.2014.08.050.
178. Shah, M. S.; Tsapatsis, M.; Siepmann, J. I. Hydrogen Sulfide Capture: From Absorption in Polar Liquids to Oxide, Zeolite, and Metal-Organic Framework Adsorbents and Membranes. *Chem. Rev.* **2017**, *117* (14), 9755–9803. https://doi.org/10.1021/acs.chemrev.7b00095.
179. Rieth, A. J.; Tulchinsky, Y.; Dincă, M. High and Reversible Ammonia Uptake in Mesoporous Azolate Metal-Organic Frameworks with Open Mn, Co, and Ni Sites. *J. Am. Chem. Soc.* **2016**, *138* (30), 9401–9404. https://doi.org/10.1021/jacs.6b05723.
180. Moghadam, P. Z.; Fairen-Jimenez, D.; Snurr, R. Q. Efficient Identification of Hydrophobic MOFs: Application in the Capture of Toxic Industrial Chemicals. *J. Mater. Chem. A* **2015**, *4* (2), 529–536. https://doi.org/10.1039/c5ta06472d.
181. Kumar, P.; Kim, K. H.; Kwon, E. E.; Szulejko, J. E. Metal-Organic Frameworks for the Control and Management of Air Quality: Advances and Future Direction. *J. Mater. Chem. A* **2015**, *4* (2), 345–361.
182. Mocniak, K. A.; Kubajewska, I.; Spillane, D. E. M.; Williams, G. R.; Morris, R. E. Incorporation of Cisplatin into the Metal-Organic Frameworks UiO66-NH2 and UiO66-Encapsulation vs. Conjugation. *RSC Adv.* **2015**, *5* (102), 83648–83656. https://doi.org/10.1039/c5ra14011k.
183. He, H.; Li, R.; Yang, Z.; Chai, L.; Jin, L.; Alhassan, S. I.; Ren, L.; Wang, H.; Huang, L. Preparation of MOFs and MOFs Derived Materials and Their Catalytic Application in Air Pollution: A Review. *Catal. Today* **2020**, *139* (February), 12125–12128. https://doi.org/10.1016/j.cattod.2020.02.033.
184. Wang, S.; Wu, D.; Huang, H.; Yang, Q.; Tong, M.; Liu, D.; Zhong, C. Computational Exploration of H2S/CH4 Mixture Separation Using Acid-Functionalized UiO-66(Zr) Membrane and Composites. *Chinese J. Chem. Eng.* **2015**, *23* (8), 1291–1299. https://doi.org/10.1016/j.cjche.2015.04.017.
185. Zhang, H. Y.; Yang, C.; Geng, Q.; Fan, H. L.; Wang, B. J.; Wu, M. M.; Tian, Z. Adsorption of Hydrogen Sulfide by Amine-Functionalized Metal Organic Framework (MOF-199): An Experimental and Simulation Study. *Appl. Surf. Sci.* **2019**, *497*, 143815. https://doi.org/10.1016/j.apsusc.2019.143815.
186. Pokhrel, J.; Bhoria, N.; Wu, C.; Reddy, K. S. K.; Margetis, H.; Anastasiou, S.; George, G.; Mittal, V.; Romanos, G.; Karonis, D.; Karanikolos, G. N. Cu- and Zr-Based Metal Organic Frameworks and Their Composites with Graphene Oxide for Capture of Acid Gases at Ambient

Temperature. *J. Solid State Chem.* **2018**, *266*, 233–243. https://doi.org/10.1016/j.jssc.2018.07.022.
187. Li, Z.; Liao, F.; Jiang, F.; Liu, B.; Ban, S.; Chen, G.; Sun, C.; Xiao, P.; Sun, Y. Capture of H2S and SO2 from Trace Sulfur Containing Gas Mixture by Functionalized UiO-66(Zr) Materials: A Molecular Simulation Study. *Fluid Phase Equilib.* **2016**, *427* (2), 259–267. https://doi.org/10.1016/j.fluid.2016.07.020.
188. Georgiadis, A. G.; Charisiou, N.; Yentekakis, I. V.; Goula, M. A. Hydrogen Sulfide (H2S) Removal via MOFs. *Materials (Basel)* **2020**, *13* (16), 12125–12128. https://doi.org/10.3390/MA13163640.
189. Ethiraj, J.; Bonino, F.; Lamberti, C.; Bordiga, S. H2S Interaction with HKUST-1 and ZIF-8 MOFs: A Multitechnique Study. *Microporous Mesoporous Mater.* **2015**, *207*, 90–94. https://doi.org/10.1016/j.micromeso.2014.12.034.
190. Shekhah, O.; Belmabkhout, Y.; Adil, K.; Bhatt, P. M.; Cairns, A. J.; Eddaoudi, M. A Facile Solvent-Free Synthesis Route for the Assembly of a Highly CO2 Selective and H2S Tolerant NiSIFSIX Metal-Organic Framework. *Chem. Commun.* **2015**, *51* (71), 13595–13598. https://doi.org/10.1039/c5cc04487a.
191. Gargiulo, N.; Peluso, A.; Caputo, D. MOF-Based Adsorbents for Atmospheric Emission Control: A Review. *Processes* **2020**, *8* (5), 12125–12128. https://doi.org/10.3390/PR8050613.
192. Zheng, C.; Shen, J.; Zhang, Y.; Huang, W.; Zhu, X.; Wu, X.; Chen, L.; Gao, X.; Cen, K. Quantitative Assessment of Industrial VOC Emissions in China: Historical Trend, Spatial Distribution, Uncertainties, and Projection. *Atmos. Environ.* **2017**, *150*, 116–125. https://doi.org/10.1016/j.atmosenv.2016.11.023.
193. Vellingiri, K.; Szulejko, J. E.; Kumar, P.; Kwon, E. E.; Kim, K. H.; Deep, A.; Boukhvalov, D. W.; Brown, R. J. C. Metal Organic Frameworks as Sorption Media for Volatile and Semi-Volatile Organic Compounds at Ambient Conditions. *Sci. Rep.* **2016**, *6*. https://doi.org/10.1038/srep27813.
194. Saha, D.; Deng, S. Structural Stability of Metal Organic Framework MOF-177. *J. Phys. Chem. Lett.* **2010**, *1* (1), 73–78. https://doi.org/10.1021/jz900028u.
195. Hua, Y.; Gargiulo, N.; Peluso, A.; Aprea, P.; Eić, M.; Caputo, D. Adsorption Behavior of Halogenated Anesthetic and Water Vapor on Cr-Based MOF (MIL-101) Adsorbent. Part II. Multiple-Cycle Breakthrough Tests. *Chemie-Ingenieur-Technik* **2016**, *88* (11), 1739–1745. https://doi.org/10.1002/cite.201600052.
196. Chakraborty, A.; Bhattacharyya, S.; Hazra, A.; Ghosh, A. C.; Maji, T. K. Post-Synthetic Metalation in an Anionic MOF for Efficient Catalytic Activity and Removal of Heavy Metal Ions from Aqueous Solution. *Chem. Commun.* **2016**, *52* (13), 2831–2834. https://doi.org/10.1039/c5cc09814a.
197. Pearson, R. G. Hard and Soft Acids and Bases. *J. Am. Chem. Soc.* **1963**, *85* (22), 3533–3539. https://doi.org/10.1021/ja00905a001.
198. Huang, Z.; Zhao, M.; Wang, C.; Wang, S.; Dai, L.; Zhang, L.; Xu, L. Selective Removal Mechanism of the Novel Zr-Based Metal Organic Framework Adsorbents for Gold Ions from Aqueous Solutions. *Chem. Eng. J.* **2020**, *384*, 123343. https://doi.org/10.1016/j.cej.2019.123343.

199. Jiang, S. Y.; He, W. W.; Li, S. L.; Su, Z. M.; Lan, Y. Q. Introduction of Molecular Building Blocks to Improve the Stability of Metal-Organic Frameworks for Efficient Mercury Removal. *Inorg. Chem.* **2018**, *57* (10), 6118–6123. https://doi.org/10.1021/acs.inorgchem.8b00704.
200. Zhang, R.; Wang, Z.; Zhou, Z.; Li, D.; Wang, T.; Su, P.; Yang, Y. Highly Effective Removal of Pharmaceutical Compounds from Aqueous Solution by Magnetic Zr-Based MOFs Composites. *Ind. Eng. Chem. Res.* **2019**, *58* (9), 3876–3884. https://doi.org/10.1021/acs.iecr.8b05244.
201. Fu, L.; Wang, S.; Lin, G.; Zhang, L.; Liu, Q.; Zhou, H.; Kang, C.; Wan, S.; Li, H.; Wen, S. Post-Modification of UiO-66-NH2 by Resorcyl Aldehyde for Selective Removal of Pb(II)in Aqueous Media. *J. Clean. Prod.* **2019**, *229*, 470–479. https://doi.org/10.1016/j.jclepro.2019.05.043.
202. Wang, C.; Lin, G.; Zhao, J.; Wang, S.; Zhang, L.; Xi, Y.; Li, X.; Ying, Y. Highly Selective Recovery of Au(III) from Wastewater by Thioctic Acid Modified Zr-MOF: Experiment and DFT Calculation. *Chem. Eng. J.* **2020**, *380* (August 2019), 122511. https://doi.org/10.1016/j.cej.2019.122511.
203. Song, J. Y.; Ahmed, I.; Seo, P. W.; Jhung, S. H. UiO-66-Type Metal-Organic Framework with Free Carboxylic Acid: Versatile Adsorbents via H-Bond for Both Aqueous and Nonaqueous Phases. *ACS Appl. Mater. Interfaces* **2016**, *8* (40), 27394–27402. https://doi.org/10.1021/acsami.6b10098.
204. Luo, Z.; Fan, S.; Liu, J.; Liu, W.; Shen, X.; Wu, C.; Huang, Y.; Huang, G.; Huang, H.; Zheng, M. A 3D Stable Metal-Organic Framework for Highly Efficient Adsorption and Removal of Drug Contaminants from Water. *Polymers (Basel)* **2018**, *10* (2), 209–222. https://doi.org/10.3390/polym10020209.
205. Abdullah, N. H.; Shameli, K.; Abdullah, E. C.; Abdullah, L. C. Solid Matrices for Fabrication of Magnetic Iron Oxide Nanocomposites: Synthesis, Properties, and Application for the Adsorption of Heavy Metal Ions and Dyes. *Compos. Part B Eng.* **2019**, *162* (December 2018), 538–568. https://doi.org/10.1016/j.compositesb.2018.12.075.
206. Li, L.; Xu, Y.; Zhong, D.; Zhong, N. CTAB-Surface-Functionalized Magnetic MOF@MOF Composite Adsorbent for Cr(VI) Efficient Removal from Aqueous Solution. *Colloids Surfaces A Physicochem. Eng. Asp.* **2020**, *586*, 124255. https://doi.org/10.1016/j.colsurfa.2019.124255.
207. Wang, K.; Tao, X.; Xu, J.; Yin, N. Novel Chitosan-MOF Composite Adsorbent for the Removal of Heavy Metal Ions. *Chem. Lett.* **2016**, *45* (12), 1365–1368. https://doi.org/10.1246/cl.160718.
208. Liu, B.; Yang, F.; Zou, Y.; Peng, Y. Adsorption of Phenol and p -Nitrophenol from Aqueous Solutions on Metal-Organic Frameworks: Effect of Hydrogen Bonding. *J. Chem. Eng. Data* **2014**, *59* (5), 1476–1482. https://doi.org/10.1021/je4010239.
209. Tella, A. C.; Owalude, S. O.; Olatunji, S. J.; Adimula, V. O.; Elaigwu, S. E.; Alimi, L. O.; Ajibade, P. A.; Oluwafemi, O. S. Synthesis of Zinc-Carboxylate Metal-Organic Frameworks for the Removal of Emerging Drug Contaminant (Amodiaquine) from Aqueous Solution. *J. Environ. Sci.* **2017**, *64* (June), 1–12. https://doi.org/10.1016/j.jes.2017.06.015.
210. Xu, G. R.; An, Z. H.; Xu, K.; Liu, Q.; Das, R.; Zhao, H. L. Metal Organic Framework (MOF)-Based Micro/Nanoscaled Materials for Heavy Metal Ions Removal: The Cutting-Edge Study on Designs, Synthesis, and Applications. *Coord. Chem. Rev.* **2021**, *427*. https://doi.org/10.1016/j.ccr.2020.213554.

211. Song, J. Y.; Jhung, S. H. Adsorption of Pharmaceuticals and Personal Care Products over Metal-Organic Frameworks Functionalized with Hydroxyl Groups: Quantitative Analyses of H-Bonding in Adsorption. *Chem. Eng. J.* **2017**, *322*, 366–374. https://doi.org/10.1016/j.cej.2017.04.036.
212. Seo, P. W.; Bhadra, B. N.; Ahmed, I.; Khan, N. A.; Jhung, S. H. Adsorptive Removal of Pharmaceuticals and Personal Care Products from Water with Functionalized Metal-Organic Frameworks: Remarkable Adsorbents with Hydrogen-Bonding Abilities. *Sci. Rep.* **2016**, *6* (September), 1–11. https://doi.org/10.1038/srep34462.
213. Lv, Y.; Zhang, R.; Zeng, S.; Liu, K.; Huang, S.; Liu, Y.; Xu, P.; Lin, C.; Cheng, Y.; Liu, M. Removal of P-Arsanilic Acid by an Amino-Functionalized Indium-Based Metal–Organic Framework: Adsorption Behavior and Synergetic Mechanism. *Chem. Eng. J.* **2018**, *339* (January), 359–368. https://doi.org/10.1016/j.cej.2018.01.139.
214. Andrew Lin, K. Y.; Yang, H.; Lee, W. Der. Enhanced Removal of Diclofenac from Water Using a Zeolitic Imidazole Framework Functionalized with Cetyltrimethylammonium Bromide (CTAB). *RSC Adv.* **2015**, *5* (99), 81330–81340. https://doi.org/10.1039/c5ra08189k.
215. Li, X.; Yuan, H.; Quan, X.; Chen, S.; You, S. Effective Adsorption of Sulfamethoxazole, Bisphenol A and Methyl Orange on Nanoporous Carbon Derived from Metal-Organic Frameworks. *J. Environ. Sci. (China)* **2018**, *63*, 250–259. https://doi.org/10.1016/j.jes.2017.10.019.
216. Bhadra, B. N.; Ahmed, I.; Kim, S.; Jhung, S. H. Adsorptive Removal of Ibuprofen and Diclofenac from Water Using Metal-Organic Framework-Derived Porous Carbon. *Chem. Eng. J.* **2017**, *314*, 50–58. https://doi.org/10.1016/j.cej.2016.12.127.
217. Bhadra, B. N.; Jhung, S. H. Adsorptive Removal of Wide Range of Pharmaceuticals and Personal Care Products from Water Using Bio-MOF-1 Derived Porous Carbon. *Microporous Mesoporous Mater.* **2018**, *270*, 102–108. https://doi.org/10.1016/j.micromeso.2018.05.005.
218. Alqadami, A. A.; Naushad, M.; Alothman, Z. A.; Ahamad, T. Adsorptive Performance of MOF Nanocomposite for Methylene Blue and Malachite Green Dyes: Kinetics, Isotherm and Mechanism. *J. Environ. Manage.* **2018**, *223* (February), 29–36. https://doi.org/10.1016/j.jenvman.2018.05.090.
219. Hasanzadeh, M.; Simchi, A.; Shahriyari Far, H. Nanoporous Composites of Activated Carbon-Metal Organic Frameworks for Organic Dye Adsorption: Synthesis, Adsorption Mechanism and Kinetics Studies. *J. Ind. Eng. Chem.* **2020**, *81*, 405–414. https://doi.org/10.1016/j.jiec.2019.09.031.
220. Torad, N. L.; Hu, M.; Ishihara, S.; Sukegawa, H.; Belik, A. A.; Imura, M.; Ariga, K.; Sakka, Y.; Yamauchi, Y. Direct Synthesis of MOF-Derived Nanoporous Carbon with Magnetic Co Nanoparticles toward Efficient Water Treatment. *Small* **2014**, *10* (10), 2096–2107. https://doi.org/10.1002/smll.201302910.
221. Shi, Z.; Xu, C.; Guan, H.; Li, L.; Fan, L.; Wang, Y.; Liu, L.; Meng, Q.; Zhang, R. Magnetic Metal Organic Frameworks (MOFs) Composite for Removal of Lead and Malachite Green in Wastewater. *Colloids Surfaces A Physicochem. Eng. Asp.* **2018**, *539*, 382–390. https://doi.org/10.1016/j.colsurfa.2017.12.043.